Final

Climate change likely increased extreme monsoon rainfall, flooding highly vulnerable communities in Pakistan

Friederike E. L. Otto[1], Mariam Zachariah[1], Fahad Saeed[2,5], Ayesha Siddiqi[3], Kamil Shahzad[4], Haris Mushtaq[5], Arulalan T[6,7], Krishna AchutaRao[7], Chaithra S T[7], Clair Barnes[1], Sjoukje Philip[8], Sarah Kew[8], Robert Vautard[12], Gerbrand Koren[9], Izidine Pinto[10,11], Piotr Wolski[11], Maja Vahlberg[10], Roop Singh[10], Julie Arrighi[10,19,20], Maarten van Aalst[10,20], Lisa Thalheimer[13], Emmanuel Raju[14], Sihan Li[15], Wenchang Yang[16], Luke J. Harrington[17], Ben Clarke[18]

1. Grantham Institute, Imperial College London, UK
2. Climate Analytics, Berlin, Germany
3. Department of Geography, University of Cambridge, UK
4. Climate Change Impact & Integration Cell (CIIC), Pakistan Meteorological Department, Pakistan
5. Center for Climate Change and Sustainable Development, Islamabad, Pakistan
6. India Meteorological Department, New Delhi, India
7. Centre for Atmospheric Sciences, Indian Institute of Technology Delhi, India
8. Royal Netherlands Meteorological Institute (KNMI), De Bilt, The Netherlands
9. Copernicus Institute of Sustainable Development, Utrecht University, Utrecht, the Netherlands
10. Red Cross Red Crescent Climate Centre, The Hague, the Netherlands
11. Climate System Analysis Group, University of Cape Town, Cape Town, South Africa
12. Institut Pierre-Simon Laplace, Paris, France
13. Center for Policy Research on Energy and the Environment, Princeton University, Princeton, USA
14. Department of Public Health, Global Health Section & Copenhagen Centre for Disaster Research, University of Copenhagen, Denmark
15. Department of Geography, University of Sheffield, UK
16. Department of Geosciences, Princeton University, Princeton, NJ 08544, USA
17. Te Aka Mātuatua School of Science, University of Waikato, Hamilton 3216, New Zealand
18. Environmental Change Institute, University of Oxford, Oxford, UK
19. Global Disaster Preparedness Center, Washington DC, USA
20. University of Twente, The Netherlands

Main findings

- The flooding occurred as a direct consequence of the extreme monsoon rainfall throughout the summer 2022 season exacerbated by shorter spikes of very heavy rain particularly in August hitting the provinces Sindh and Balochistan. We therefore consider 60-day and 5-day maximum rainfall during the monsoon season for the Indus basin and the two provinces respectively.

- The devastating impacts were also driven by the proximity of human settlements, infrastructure (homes, buildings, bridges), and agricultural land to flood plains, inadequate infrastructure, limited ex-ante risk reduction capacity, an outdated river management system, underlying vulnerabilities driven by high poverty rates and socioeconomic factors (e.g. gender, age, income, and education), and ongoing political and economic instability.

- The return time for both events defined above is about 1 in 100 years in today's climate. Rainfall in the Indus basin is however extremely variable from year to year, due to, amongst other drivers, the strong correlation with the ENSO cycle. Thus, exact quantification is difficult.

- First, looking just at the trends in the observations, we found that the 5-day maximum rainfall over the provinces Sindh and Balochistan is now about 75% more intense than it would have been had the climate not warmed by 1.2C, whereas the 60-day rain across the basin is now about 50% more intense, meaning rainfall this heavy is now more likely to happen. There are large uncertainties in these estimates due to the high variability in rainfall in the region, and observed changes can have a variety of drivers, including, but not limited to, climate change.

- Secondly, to determine the role of human-induced climate change in these observed changes we looked at the trends in climate models with and without the human-induced increases in greenhouse gases. The regions involved are at the western extreme end of the monsoon region, with large differences in rainfall characteristics between dry western and wet eastern areas.

- Many of the available state-of-the-art climate models struggle to simulate these rainfall characteristics. Those that pass our evaluation test generally show a much smaller change in likelihood and intensity of extreme rainfall than the trend we found in the observations. This discrepancy suggests that long-term variability, or processes that our evaluation may not capture, can play an important role, rendering it infeasible to quantify the overall role of human-induced climate change.

- However, for the 5-day rainfall extreme, the majority of models and observations we have analysed show that intense rainfall has become heavier as Pakistan has warmed. Some of these models suggest climate change could have increased the rainfall intensity up to 50% for the 5-day event definition.

- Looking at the future, for a climate 2 °C warmer than in preindustrial times, models suggest that rainfall intensity will significantly increase further, for the 5-day event, while the uncertainty remains very large for the 60-day monsoon rainfall.

- Our results are in alignment with recent IPCC reports.

- Both current conditions and the potential further increase in extreme peaks in rainfall over Pakistan in light of human-caused climate change, suggest that there is an urgent need to reduce vulnerability to extreme weather in Pakistan.

1 Introduction

From mid-June 2022, large areas of Pakistan experienced record-breaking monsoonal rainfall, falling in several pulses, until late August. By the end of August large parts of the country were submerged. The Indus river, that runs the length of the country, burst its banks across thousands of square kilometres, while the intense rainfall also led to urban flash floods, landslides and Glacial Lake Outburst Floods (OCHA, 2022a). Due to the Indus overflowing, a 100-km wide lake was created in the southern province of Sindh, which together with the neighbouring province of Balochistan constituted the worst affected region in the country. The record rainfall that fell between 1st-31st August over Sindh and Balochistan were 726% and 590% of the usual totals for August in the respective regions (Business Recorder, 2022). Pakistan as a whole received 243% more rainfall than usual during this period, and stands as record wettest August since records began in 1961 (PMD, 2022). This exceptionally high monsoon precipitation hit a country with both high population density and high rates of poverty, creating significant vulnerability to climate-related hazards and potential changes in likelihood and intensity of such events. The flooding affected over 33 million people, destroyed 1.7 million homes, and nearly 1500 people died (NDMA, 2022; VOA News, 2022). On August 25th, the government declared a national emergency. Damages likely exceed preliminary estimates of around US$30 billion with further economic disruption certain in the months to come (Business Standard, 2022). 6700 kilometres of road, 269 bridges and 1460 health facilities were destroyed (OCHA, 2022b), 18590 schools

damaged (Save the Children, 2022), 750,000 livestock were killed (NDMA, 2022) and around 18,000 square kilometres of cropland were ruined, including roughly 45% of the cotton crop (Bloomberg, 2022a) – one of the nation's key exports. The loss of food crops, totalling around US$2.3 billion (Bloomberg, 2022b), also compounds the ongoing food shortages due to the war in Ukraine and summer heatwaves in the region. There is also a severely heightened risk of the spread of disease, as stagnant flood waters provide a breeding ground for pathogens, and the vast number of people displaced results in poor hygiene and sanitation in temporary accommodation (Sarkar, 2022; Baqir et al., 2012). Notably, across Sindh and Balochistan, there has been an outbreak in waterborne disease such as diarrhoea and cholera, as well as skin and eye infections, malaria, and fever (IRC, 2022).

1.1 The meteorological event

Pakistan is on the far western edge of the South Asian monsoon region, with a mostly arid desert climate in the southern provinces and humid to the north (Ahmed et al., 2019). From June-September, Pakistan often receives heavy rainfall, especially in the northern parts of the country, with over half a million people affected by flooding annually (Baqir et al., 2012). However, it is usually not affected by monsoon low pressure systems, and generally receives far less rainfall than parts of India at the same latitudes. As a result, precipitation rates in Pakistan are extremely variable (Adnan et al., 2021; Ali et al., 2020). Past intense monsoons in both India and Pakistan are linked to strong La Niña events (Safdar et al., 2019; Ju & Slingo, 1995).

In 2022, a La Niña event combined with a confluence of other factors to extend and intensify the monsoon over Pakistan, resulting in severe flooding. Unusually hot weather in spring and through the summer in Pakistan enhanced an intense depression from the Arabian Sea, bringing heavy rainfall to the southern regions (Mallapaty, 2022). In the months of March and April 2022, an atypical time of year to witness severe heat, temperatures rose to more than 50°C in some parts of the country, incurring various damages including wheat yield and livestock losses, forest fires, damage to infrastructure, and health issues. The hot summer also amplified the melting of Pakistan's 7000 glaciers that feed the Indus river (NASA Earth Observatory, 2022), though the relative contribution of glacial meltwater to the flooding is unknown (Mallapaty, 2022) and likely much smaller than the rainfall itself.

Before 2022, the biggest flooding event faced by the country was in 2010, which impacted an estimated 14-20 million people and killed over 1,700. Nearly 1.1 million homes and 436 health care centres were destroyed or damaged (World Food Programme, Sept 2010). The flooding caused US$9.7 billion in damages in 46 of the country's 135 districts. The rural economy was severely impacted, including agriculture, fertilisers, agricultural machinery, livestock, animal sheds, personal seed stocks, fisheries and forestry. Infrastructure losses were widespread, damaging 2.9 million households and 80% of the national food reserve

(Polastro et al., 2011). This year's monsoon season is not over yet and the scale of destruction from the flooding is already expected to be far higher than 2010.

In 2010, the flooding was triggered by a trough in the upper atmosphere associated with the mid-latitude jet-stream (Scott, 2010). The presence of a mid latitude westerly trough aloft in the north and low level moisture feeding through monsoon flow along the Himalayas and also the direct south-westerly current from the Arabian Sea resulted in the heavy downpour in the northern part of the country from 28-30 July. This event resulted in the catastrophic riverine flooding that started from the northern part of the Indus basin. Since the Indus basin traverses Pakistan from north to south and nearly bisects the physical territory of the country longitudinally, the 2010 floods impacted a large portion of the country, particularly the regions along the river banks.

Fig. 1 presents three different flood-producing mechanisms during the monsoon season in Pakistan at climatological time scale. Category-I floods are normally caused by the advection of moisture from the Bay of Bengal and the Arabian Sea, associated with the dynamical features in the atmosphere, such as the mid-latitudinal jet stream. Category-II floods are caused by the movement of monsoonal depressions originating in the Bay of Bengal and travelling over the Indo-Gangetic plains, thereby causing rainfall over the eastern upper Indus basin. Category-III floods are the most severe, caused by monsoon depressions over the Bay of Bengal travelling over central India. After reaching the states of Gujarat and Maharashtra, these depressions move towards the western upper Indus basin after receiving moisture from the Arabian Sea. In all three flood-producing mechanisms, orography in the upper Indus basin plays a very important role along with the upper air circulation associated with the mid-latitude jet stream.

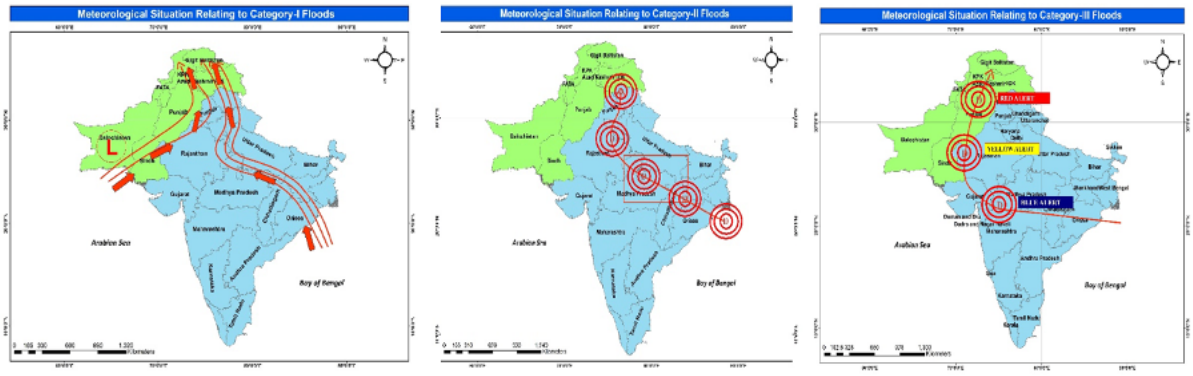

***Figure 1**: Schematic diagram of three flood bearing mechanisms during summer monsoon season (source: Pakistan Meteorological Department)*

Unlike 2010, the 2022 monsoon season received multiple depressions from Bay of Bengal in the months of July and August, which particularly impacted the two southern provinces of Sindh and Balochistan. Figure 3 shows 8 tracks of monsoon depression observed during the 2022 season, sourced from the Pakistan Meteorological Department (PMD). Whereas

monsoon depressions generally travel towards the northern part of the country during the monsoon season, all 8 tracks were directed towards the southern provinces of Sindh and Balochistan this year, resulting in more than 500% of climatological rainfall during the two months of July and August, relative to their long-term average.

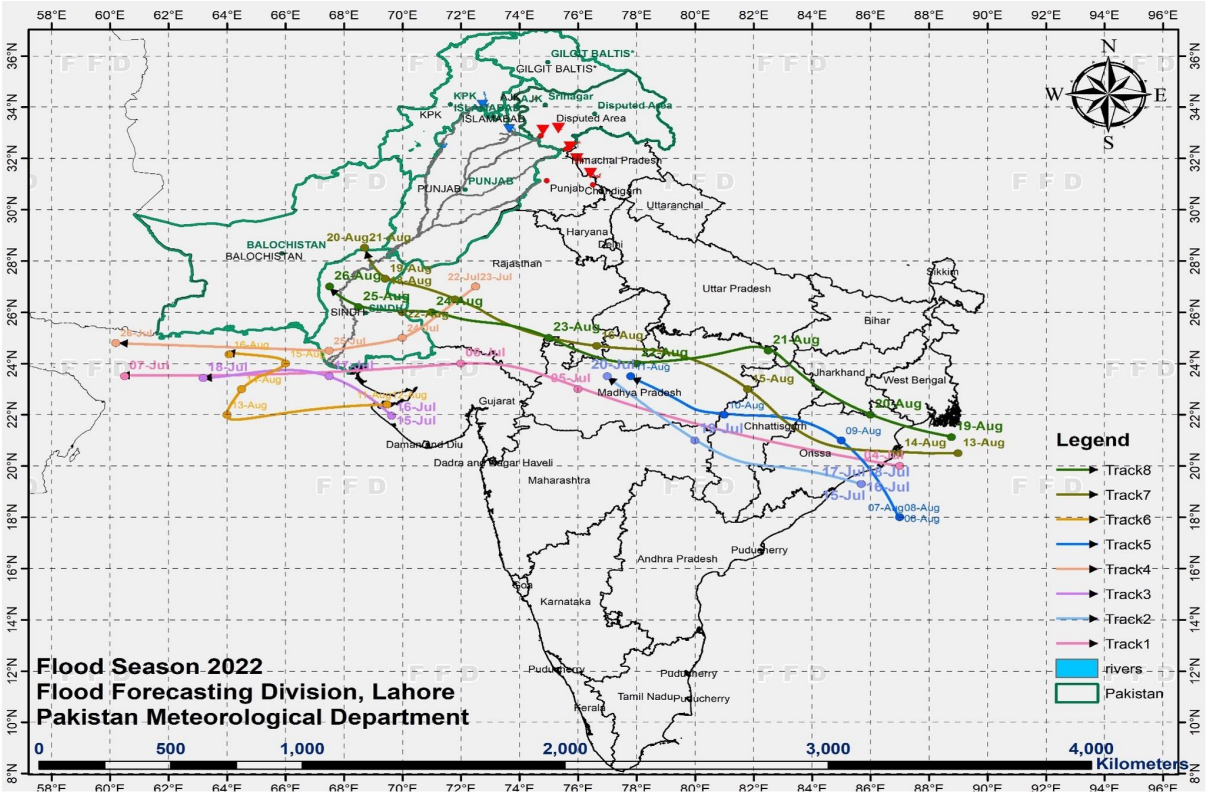

***Figure 2**: Movement of monsoon depressions from Bay of Bengal across India and Pakistan during the monsoon season 2022 (source:Pakistan Meteorological Department)*

1.1.1 Role of La Niña

A commonality between the 2010 and 2022 events exists in the form of the occurrence of La Niña in the tropical central Pacific. Fig. 3 (*right*) shows that the La Niña pattern was more intense in 2010 compared to 2022. However, unlike 2010, a negative Indian Ocean Dipole (IOD) exists in 2022, as shown in Fig. 3 (*left*). Concurrence of La Niña and negative IOD during 2022 indicates anomalous warmer sea surface conditions in the eastern Indian ocean (around Indonesia), thus providing additional moisture to feed monsoon depressions. Fig. 4 shows the correlation between Jul-Aug precipitation in the CPC dataset averaged over the Indus basin and the NCDCv5 ERSST Sea Surface Temperature (SST) values (Huang et al., 2017). The strong correlation over the NINO 3.4 region suggests that the strong La Niña has indeed exaggerated the precipitation over the Indus basin.

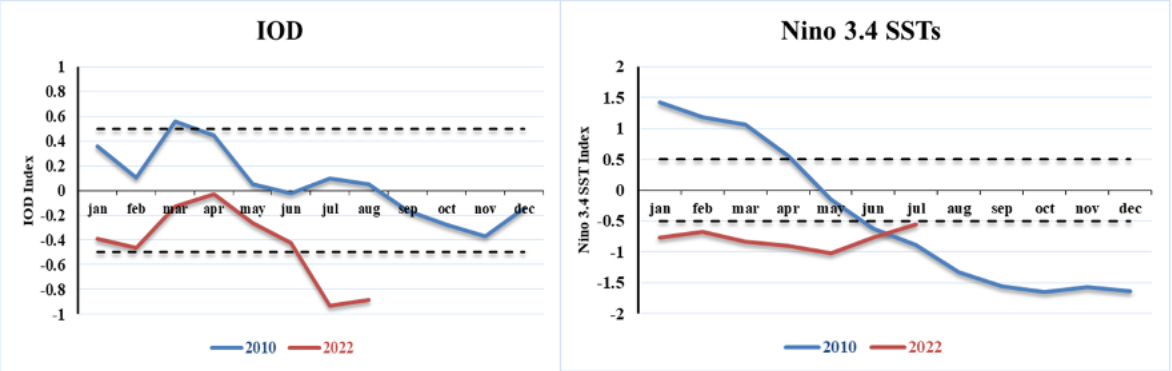

***Figure 3**: Comparison of La Niña (Nino 3.4 index) and IOD between 2010 and 2022 flooding events*

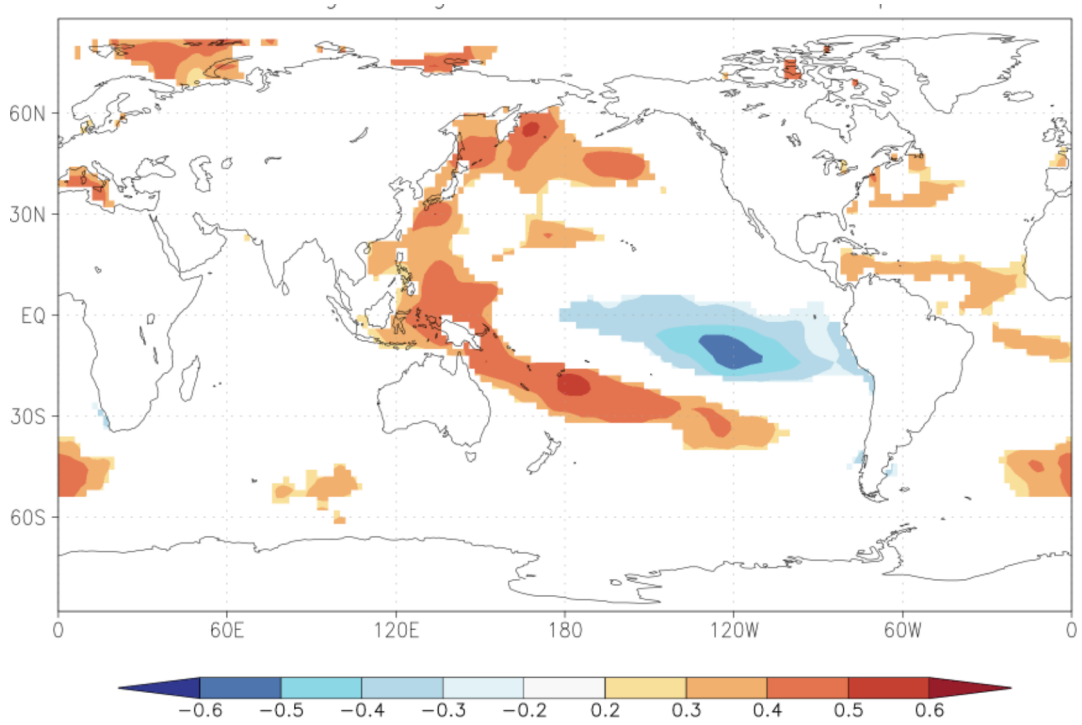

***Figure 4**. Correlation between rainfall (CPC dataset) over Jul-Aug in the Indus basin and global ERSST Sea Surface Temperatures for months Jul-Aug, calculated over years 1979-2022.*

1.1.2. Role of Heat Low over Pakistan

Heat lows during the month of May over Pakistan are found to be associated with excessive precipitation in the following monsoon season (Bansod and Singh, 1995). Fig. 5 shows the anomalies in mean sea level pressure and the 2m-temperature in the month of May, for the years 2010 (Fig. 5 (*left*)) and 2022 (Fig. 5 (*right*)) over a larger region covering India and Pakistan. The anomalies for 2022 May (Fig. 5 (*right*)) suggests that the high surface temperatures may have led to the intensification of the heat low over Pakistan, which in turn

may have influenced the migration of monsoon depressions toward the southern provinces-Balochistan and Sindh.

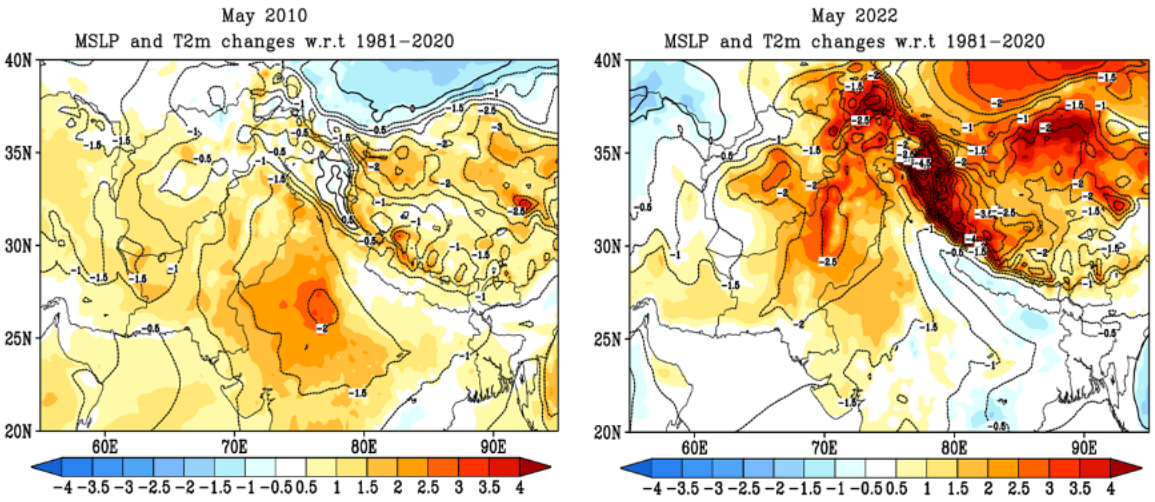

***Figure 5**: 2m Temperature (shaded) and mean sea level pressure (isobars) anomalies from ERA5*

It is worth mentioning here that a study carried out by World Weather Attribution (2022) earlier this year concluded that climate change made that particular heat wave 30 times more likely as compared to the pre-industrial world.

1.1.3 Role of Mid-Latitude Jet Stream

It is well established that in 2010, a blocking event in the jetstream occurred, which caused a simultaneous occurrence of a heatwave in Russia (Met Office, n.d.) and flooding in Pakistan.

In 2022, in addition to the monsoon depression received by the southern provinces of Sindh and Balochistan, the northern province of Khyber Pakhtunkhwa (KPK) and north western Balochistan received heavy rainfall towards the end of August (shown by red circles in the right hand panel of Figure 6) which was not connected with the monsoon disturbances discussed earlier, and was speculated to be associated with the mid-latitude jet stream. This particular downpour in KPK resulted in the Indus riverine flooding which continued untilSeptember in the downstream Indus river.

To explore the difference in the patterns of rainfall events further, we looked at two separate events in 2022 August. An event from 18th to 19th August which caused heavy rainfall in Sindh, and another spell resulting in high level of rainfall in KPK and western Balochistan from 25th to 27th August as shown by the red circles in Figure 6. While it is evident that the 18th-19th event over Sindh occurred because of monsoon depressions, the other event over KPK and western Balochistan cannot be explained by the tracks in Figure 2. We compared the atmospheric patterns leading to the two events along with its comparison with the 28-30 July 2010 event.

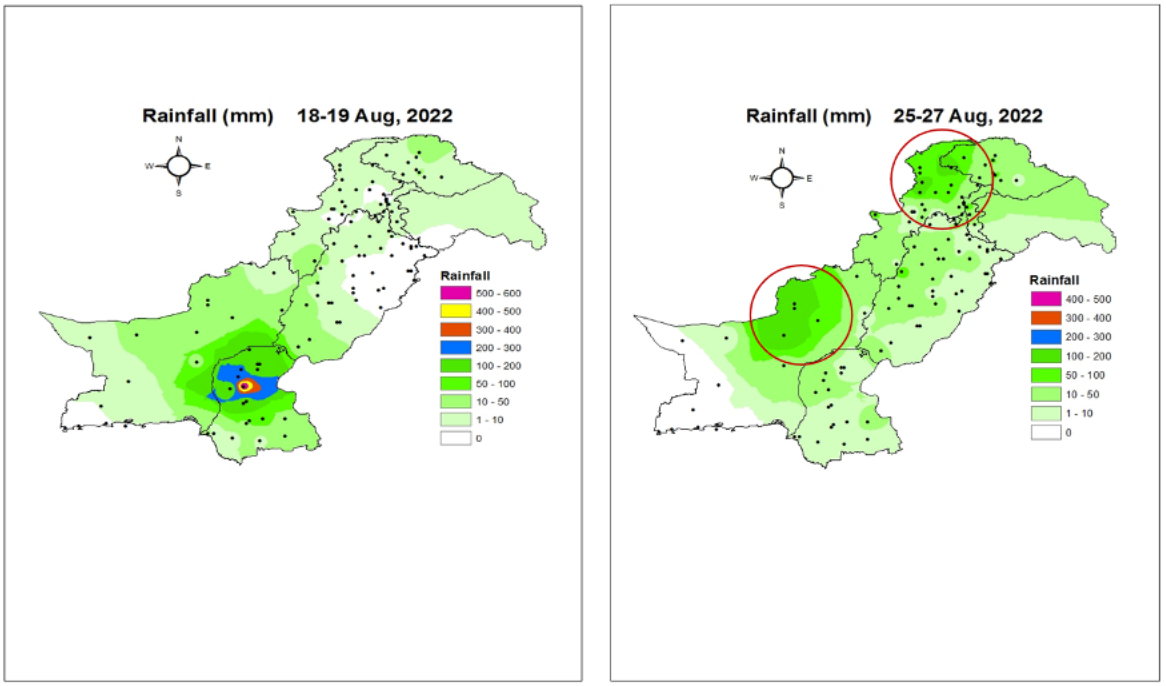

***Figure 6**: Rainfall for the two events from Pakistan Meteorological Department Data*

Figure 7 shows the upper tropospheric circulation for the three events at 200 hPa. The 2010 event corresponds very well with the 25-27 August 2022 event, with both having a prominent trough over Afghanistan and the trough exit region lying over Pakistan including KPK and north-western Balochistan. However, the trough-like pattern associated with the jet stream is simply missing for the 18-19 August event. This implies that similar to the 2010 event, 25-27 August 2022 rainfall event can be attributed to the trough associated with the mid-latitude jet stream.

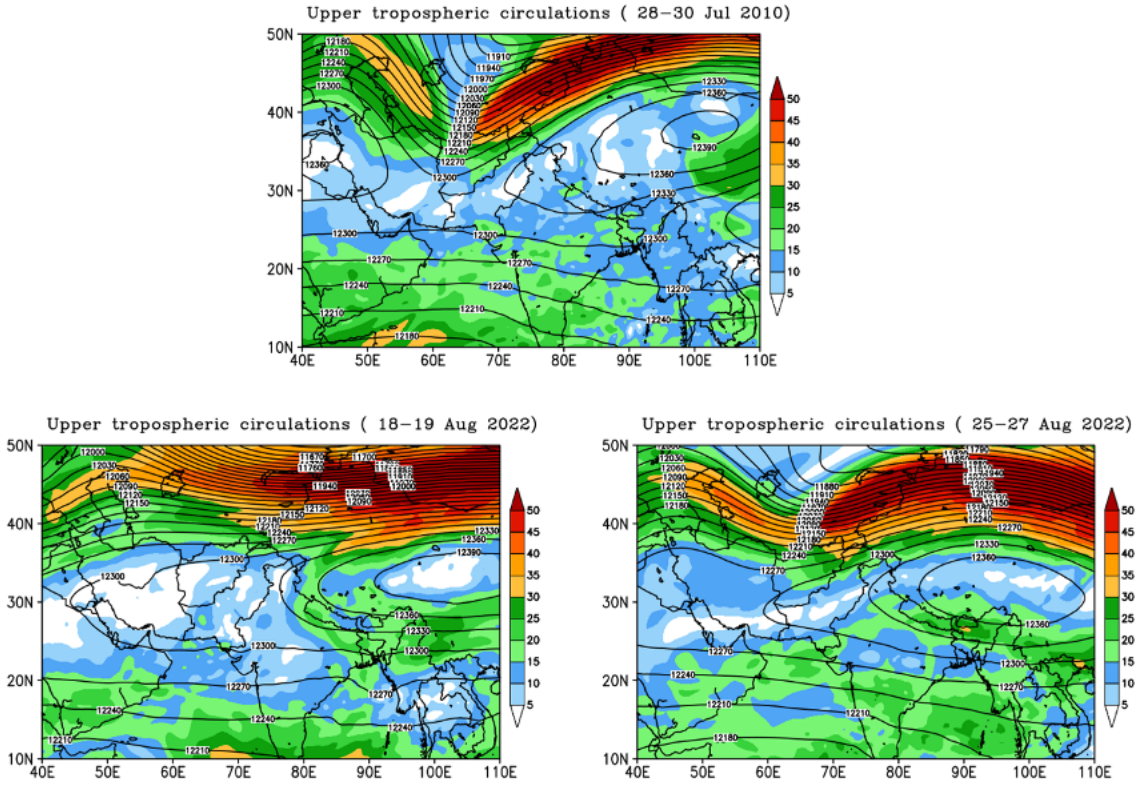

***Figure** 7: 200 hPa geopotential heights (isobars) and wind speed (unit; meter/second, shaded) from ERA5 data*

1.2 Event Definition

Taking this analysis into account and considering that the atmospheric conditions leading to rainfall in the southern provinces is different from the northern part of the country, we analyse the 2022 event over two regions: (i) the whole Indus basin as shown by the red highlight in Fig. 8(a) and (ii) a region combining the southern provinces of Sindh and Balochistan (Fig. 8(b)). We also use two different temporal scales to distinguish the long-duration core of the monsoon season and the acute episodes above mentioned. This distinction is also motivated by differences in the corresponding physical and dynamical mechanisms.

The two event definitions for the remainder of this study are: (1) annual maximum of the mean 60-day precipitation during June-September, over the Indus river basin (Fig. 8 (a)) (the core of the monsoon rainfall season), and (2) the annual maximum of the mean 5-day precipitation in June-September over the Sindh and Balochistan provinces together (Fig. 8(b)) (the most extreme spell). These two metrics align most closely with the impacts of the event, capturing both the short heavy precipitation in the southern provinces, as well as the longer spell over Pakistan.

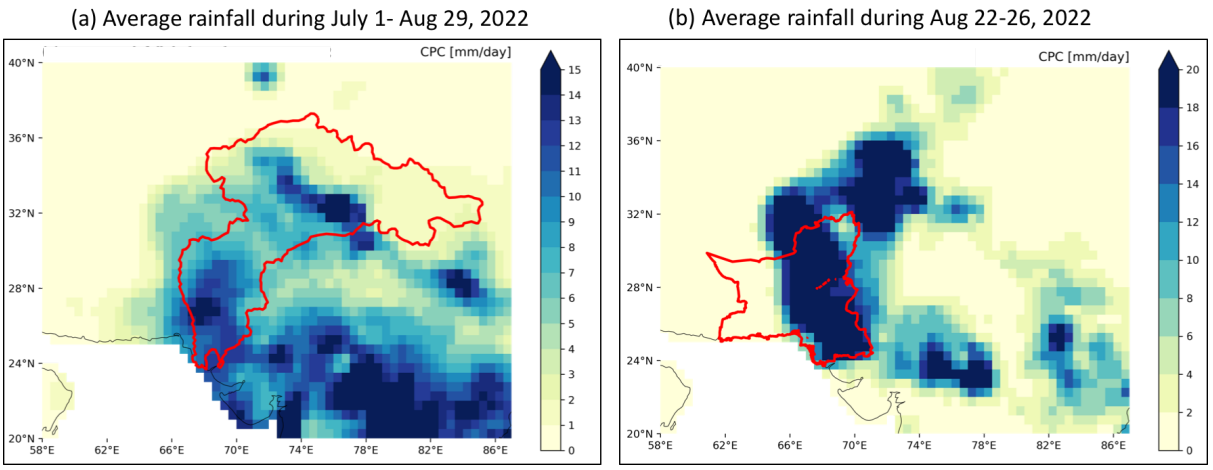

***Figure 8**. a) Observed average 60-day rainfall for 1 July -29 Aug 2022. The red highlight shows the Indus river basin (b) 5 -day rainfall for 22-26 Aug, 2022. The study region encompassing Balochistan and Sindh is highlighted in red*

1.3 Similar events in the scientific literature

Pakistan is one of the countries that are most at risk of climate extremes according to German Watch (2021). It is located at a place where two precipitation bearing weather systems terminate- the monsoon rains from east and south east during summer, and the westerly disturbances from the Mediterranean Sea during winter. It is well established that climate change results in increasing the variability of these systems (Douville et al., 2021). These changes, either spatially or temporally, make the country more prone to such extremes. Being a low-middle income country, Pakistan has low readiness despite its high vulnerability. The Notre Dame Global Adaptation index ranks Pakistan 32nd least ready country out of 181 to tackle climate change.

The country has a largely arid desert climate and frequently experiences severe heatwaves, such as the event in early summer 2022 that was strongly amplified by anthropogenic climate change (WWA, 2022). It also periodically experiences destructive rainfall-induced flood events, as occurred in 2010. There is strong evidence of an increasing trend in extreme rainfall in South Asia (IPCC, 2021) and an increasing strength and westward movement of the monsoon over Pakistan (Hanif et al., 2013). However, there is low confidence that the observed extreme rainfall increase is due to human influence on the climate system (IPCC, 2021), partially because other factors are known to influence monsoon strength, such as irrigation practices (Devanand et al., 2019).

Previous attribution studies for the heavy rainfall of 2010 (responsible for massive flooding) have been undertaken, each using only a single model. Christidis et al. (2013) found that the model used could not accurately reproduce such events. Meanwhile, Hirabayashi et al. (2021) found an increase due to anthropogenic climate change, but the model was not assessed for its

robustness in simulating monsoon dynamics. In a recent study, Di Capua et al. (2021) showed that the 2010 rainfall in Pakistan and the heatwave in Russia in the same year were connected by a wave train, which in turn was driven by sea surface temperature anomalies, soil moisture deficits in the extratropical regions and land surface warming in the high-latitudes. All or some of these drivers could be influenced by anthropogenic climate change, but whether and the extent to which this is the case remains highly uncertain. All of these studies thus underline the importance of (i) understanding the rainfall mechanisms and the factors that influence them including climate change, and (ii) the reliability of climate models in capturing them. Therefore, at present, there is overall low confidence in existing attribution findings for this region.

Meanwhile, projections indicate a rapid rise in the intensity of extreme precipitation events in the wider region including Pakistan with further global warming (IPCC, 2021), linked to a stronger and more variable Indian monsoon (Katzenberger et al., 2022; Katzenberger et al., 2021). It is however important to highlight that these projections are conducted for a larger region including India, which has much less variable monsoon rains, and thus are not designed to specifically inform future changes in heavy rainfall over the region flooded in 2022.

2 Data and methods

2.1 Observational data

Daily rainfall data for 47 stations from 1961- 2017 were made available by Pakistan Meteorological Department (PMD). The station locations can be found here. We limit this data to evaluating the performance of the various gridded datasets that are considered for this analysis.

We use three gridded datasets for fitting probability distributions to rainfall in the study domains and thereafter analysing the heavy rainfall event of 2022 in the context of climate change. The first dataset is the gridded dataset of daily rainfall known as the CPC Global Unified Gauge-Based Analysis of Daily Precipitation data, that is provided by the NOAA PSL, Boulder, Colorado, USA, from their website. This data is available at 0.5° x 0.5° resolution, for the period 1979-present. The second dataset is the European Centre for Medium-Range Weather Forecasts' ERA5 reanalysis product, which is longer in length (starting at 1950). We note that precipitation from ERA5 is not directly assimilated, but is a diagnostic variable generated by atmospheric components of the IFS modelling system. We use the satellite-based GPM-IMERG data product as the third dataset. This product uses the Integrated Multi-satellitE Retrievals for GPM (IMERG) algorithm for combining information from the GPM satellite constellation to estimate precipitation over the majority of the Earth's surface (Rozante et al. 2010).

Fig. 9 shows the time series of the JJAS rainfall averaged over Pakistan (Fig. 9(a)) and over the southern provinces of Balochistan and Sindh (Fig. 9(b)). In general, all three gridded datasets are found to match the observed variability in the station-based averages. However, due to inconsistencies among the three datasets in length, trends and the magnitude of the 2022 event, we use all three datasets for evaluating the observed trends and return times that are subsequently used for climate model evaluation (discussed in section 4).

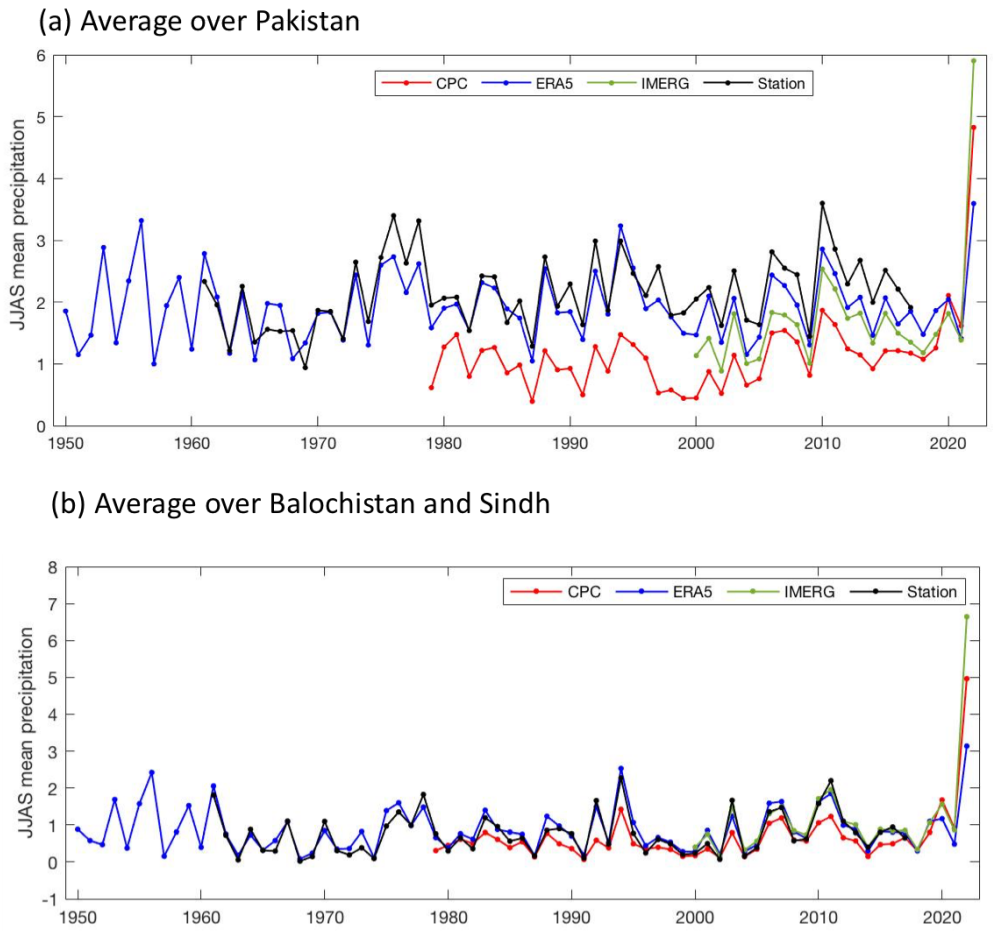

Figure 9. Comparison of the datasets used in this study with the station averages for (a) Pakistan as a whole and (b) the southern region consisting of Balochistan and Sindh provinces.

Finally, as a measure of anthropogenic climate change, we use the (low-pass filtered) global mean surface temperature (GMST), where GMST is taken from the National Aeronautics and Space Administration (NASA) Goddard Institute for Space Science (GISS) surface temperature analysis (GISTEMP, Hansen et al., 2010 and Lenssen et al. 2019).

2.2 Model and experiment descriptions

We used the available model simulations from the COordinated Regional Downscaling EXperiment (CORDEX) over South Asia with the historical period usually starting in 1950 (or 1970) and ending in 2005, followed by the RCP8.5 scenario until 2050. The simulations are made with regional climate model (RCM) simulations downscaling global climate model (GCM) simulations. On total, 24 simulations were used for both indices, with 2 resolutions: 0.44° (about 50 km) (16 models) and 0.22° (about 25 km) (8 models). The domain encompasses a wide area with Himalaya Mountain range and a large area of the Indian Ocean to allow the full monsoon systems to be included. The CORDEX projections for South Asia have been used in a number of studies (see e.g. Rai et al., 2019; Suman and Maity, 2020; Singh et al., 2020; Senatore et al., 2019), including the attribution study of the India/Pakistan heat in March/April 2022 (see https://www.worldweatherattribution.org). CORDEX simulations, as well as global scale simulations, have been shown not to reproduce well the South Asian precipitation climatology (see e.g. references in the AR6 WGI IPCC Chapter Atlas report, Gutiérrez et al., 2021). The impact of a higher resolution has however shown some improvement (Mishra et al., 2020). We provide a specific assessment for the Pakistan case below.

The second ensemble considered in this study is GFDL-CM2.5/FLOR. This is a fully coupled climate model developed at the Geophysical Fluid Dynamics Laboratory (GFDL; Vecchi et al., 2014) with horizontal resolution of 50 km for land and atmosphere and 1 degree for ocean and ice. The ten ensemble simulations cover the period from 1860 to 2100, and include both the historical and RCP4.5 experiments driven by transient radiative forcing from CMIP5 (Taylor et al., 2012).

We also use the HighResMIP SST-forced model ensemble (Haarsma et al. 2016), the simulations for which span from 1950 to 2050. The SST and sea ice forcings for the period 1950-2014 are obtained from the 0.25° x 0.25° Hadley Centre Global Sea Ice and Sea Surface Temperature dataset that are area-weighted regridded to match the climate model resolution (see Table 1). For the 'future' time period (2015-2050), SST/sea-ice data are derived from RCP8.5 (CMIP5) data, and combined with greenhouse gas forcings from SSP5-8.5 (CMIP6) simulations (see Section 3.3 of Haarsma et al. 2016 for further details).

2.3 Statistical methods

In this analysis we analyse time series from the Indus basin (Fig. 8(a)) and the combined provinces of Sindh and Balochistan (Fig 8(b)) of daily precipitation values where long records of observed data are available. Methods for observational and model analysis and for model evaluation and synthesis are used according to the World Weather Attribution Protocol, described in Philip et al. (2020), with supporting details found in van Oldenborgh et al. (2021), Ciavarella et al. (2021) and here.

The analysis steps include: (i) trend calculation from observations; (ii) model validation; (iii) multi-method multi-model attribution and (iv) synthesis of the attribution statement.
We calculate the return periods, Probability Ratio (PR; the factor-change in the event's probability) and change in intensity of the event under study in order to compare the climate of now and the climate of the past, defined respectively by the GMST values of now and of the preindustrial past (1850-1900, based on the Global Warming Index https://www.globalwarmingindex.org). To statistically model the event under study, we use a GEV distribution that scales with GMST for both the 5-day and the 60-day event definitions. Next, results from observations and models that pass the evaluation tests are synthesised into a single attribution statement.

3 Observational analysis: return period and trend

3.1 Analysis of gridded data

Fig.10 shows the annual precipitation time-series for CPC (1979-present; *left)*, ERA5 (1950-present; *middle*) and IMERG (2000-present; *right*) for the Indus river basin (Fig. 10 (a)) and the smaller region of Balochistan and Sindh (Fig. 10 (b)). Overall, these records are in agreement, however, due to the shorter length of the CPC and IMERG datasets and inconsistencies in the magnitude of the 2022 event among the three datasets, it is difficult to select one of these as the primary data. We thus use all three datasets (Fig. 10) for computing observed return periods of the events and synthesis, and CPC and ERA5 for model evaluation.

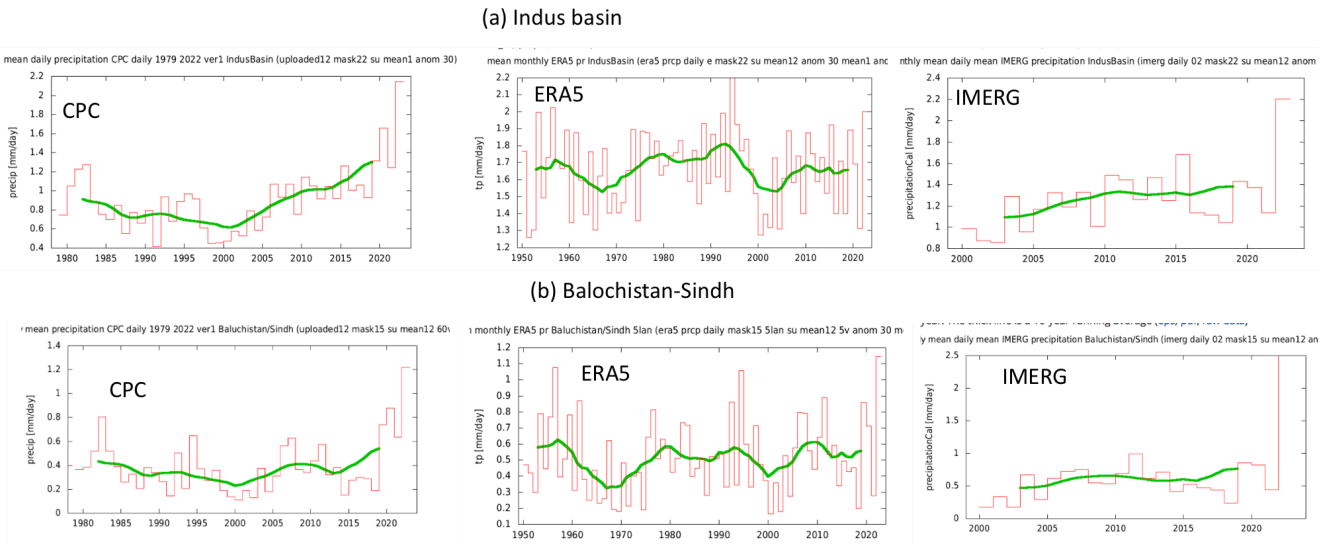

Figure 10. *Time series of annual average rainfall (mm/day) along with the ten-year running mean (shown by green line) for (a) the Indus river basin and (b) the southern provinces of*

Balochistan and Sindh (bottom), based on CPC (left), ERA5 (middle) and IMERG (right) rainfall datasets.

The left panels in Fig. 11 show the response of JJAS maximum of 60-day average precipitation to the global mean temperature, for the Indus river basin, based on the gridded CPC, ERA5 and IMERG datasets. The right panels in Fig. 11 show the return period curves in the present, 2022 climate and the past climate when the global mean temperature was 1.2 °C cooler. We find that the return period of the maximum 60-day rainfall over the Indus Basin in JJAS 2022 in the 2022 climate is consistent across all datasets, ranging from 85-96 years. We round this to 100 years for the remainder of the analysis.

Similar plots for the JJAS maximum 5-day average rainfall in the southern provinces of Balochiostan and Sindh are shown in Fig. 12. The return periods of this event in the current, 2022 climate are also found to closely match in all of the datasets (right panels in Fig. 12), again the return period is rounded to 100 years for the rest of the analysis.

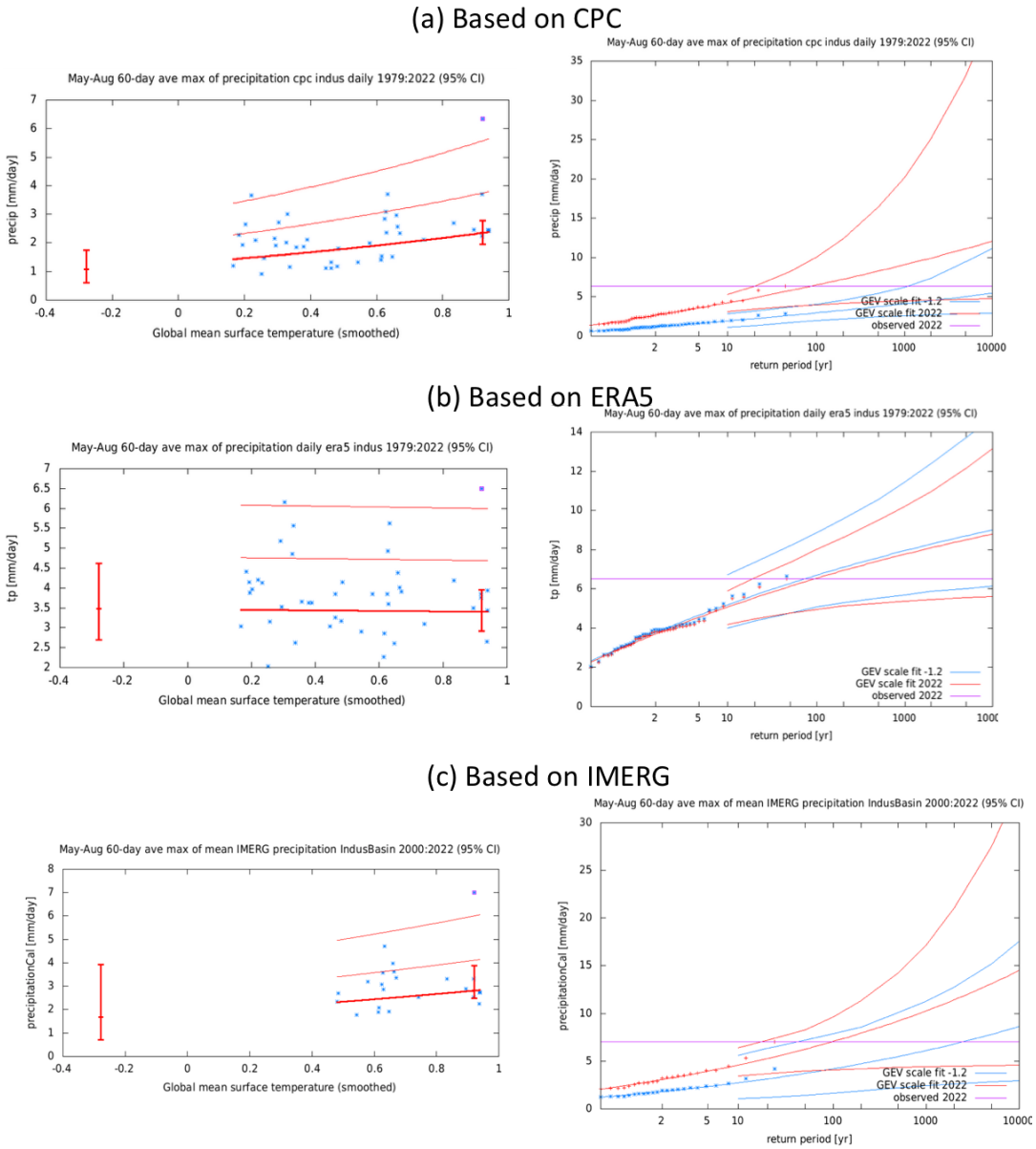

Figure 11. *GEV fit with constant dispersion parameters, and location parameter scaling proportional to GMST of the index series, for the Indus river basin based on three gridded datasets- (a) CPC (b) ERA5 and (c) IMERG. The 2022 event is included in the fit.* ***Left****: Observed max. 60-day average rainfall in the JJAS season as a function of the smoothed GMST. The thick red line denotes the time-varying location parameter. The vertical red lines show the 95% confidence interval for the location parameter, for the current, 2022 climate and a 1.2ºC cooler climate. The 2022 observation is highlighted with the magenta box.* ***Right****: Return time plots for the climate of 2022 (red) and a climate with GMST 1.2 ºC cooler (blue). The past observations are shown twice: once shifted up to the current climate and once shifted down to the climate of the late nineteenth century. The markers show the data and the lines show the fits and uncertainty from the bootstrap. The magenta line shows the magnitude of the 2022 event analysed here.*

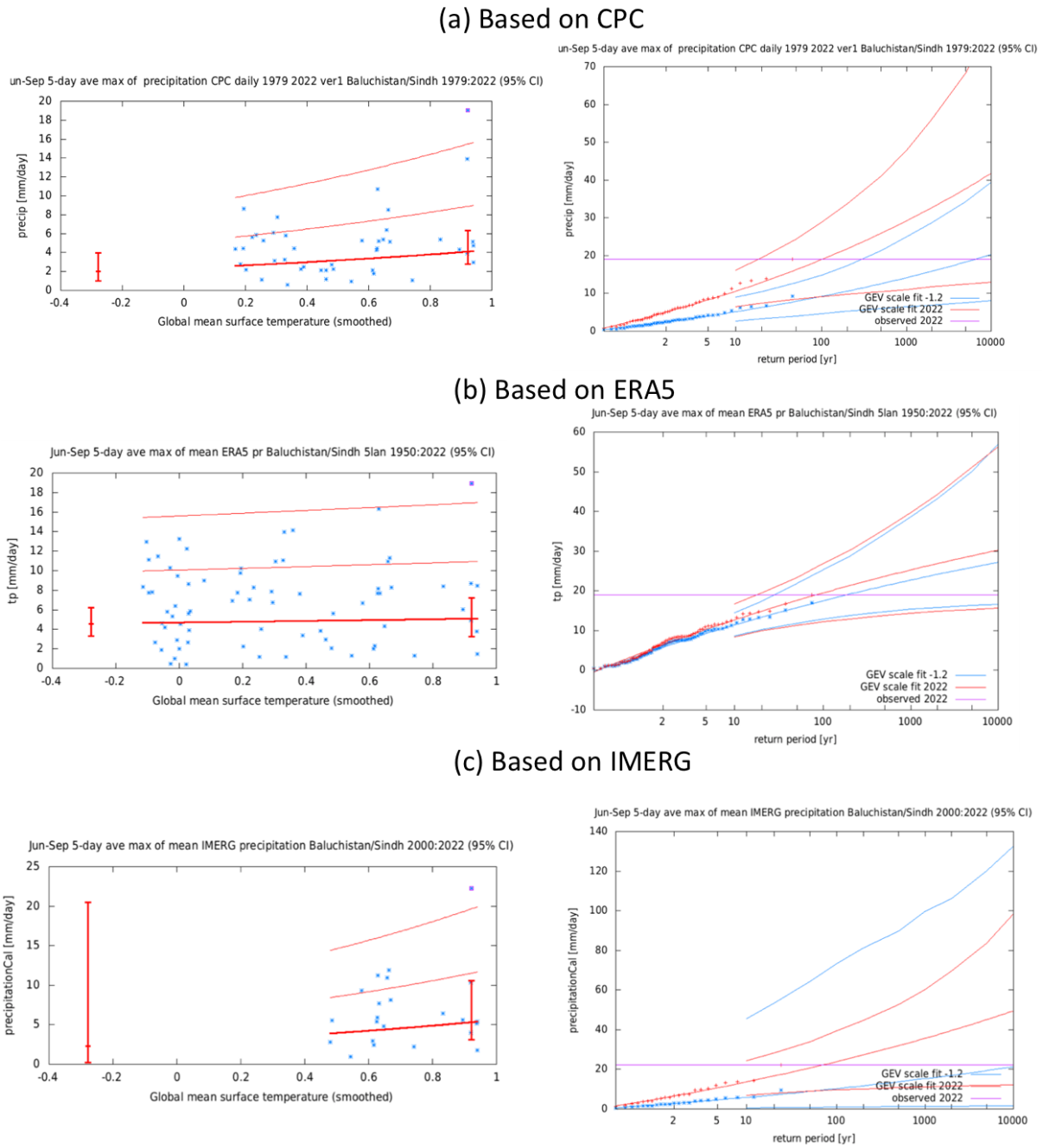

Figure 12. *same as Fig. B, for the region encompassing the southern provinces of Balochistan and Sindh based on (a) CPC (b) ERA5 and (c) IMERG datasets.*

4 Model evaluation

In the subsections below we show the results of the model evaluation for the two event definitions. Per framing or model setup we use both the good and reasonable models. The tables show the model evaluation results. The model evaluation and selection is carried out by verifying the following elements:

- Satisfactory seasonal cycles for the index used (here, rainfall averaged over the Indus basin and over the Southern regions), with an emphasis on capturing the monsoon peak in the right months (from July to September);
- Satisfactory spatial patterns of mean rainfall during the central monsoon months (July and August), capturing the West-East gradient of mean rainfall over Pakistan;
- Model fit parameter (dispersion and shape) confidence intervals that overlap with those from observations. For the observations we pooled the two confidence intervals of ERA5 and CPC, by taking the lowest and highest values of the two 95% confidence intervals to represent the observational uncertainty range;
- In addition, we checked the bias of the magnitude corresponding to a 100 year return value for models.For the case of the 5-day event definition, rainfall totals corresponding to a 100-year return value exhibited large positive biases in some models (eg. more than twice the observed value), in which case they were discarded.

4.1 Indus Basin

The Indus basin is located in the gradient of monsoon rainfall climatology, which makes results sensitive to the representation of the monsoon location in models. As a result, many models fail to reproduce one of the characteristics used for model evaluation. For CORDEX overall, among the 24 models tested, only 17 are selected. For the low-resolution ensemble (0.44°) the capacity of the fit parameters to reproduce observations is highly dependent on the regional climate model, the RCA model having a better skill over the RegCM model in general. For the higher resolution ensemble (0.22°) the parameters better fit the observations. In some cases the seasonal cycle was shifted toward much more rain during the winter months and sometimes without a monsoon signal. The FLOR ensemble could not be selected as it was unable to reproduce the statistical fit parameters. Out of the six HighResMIP models that were tested for the study, we selected four models that sufficiently capture the seasonal and spatial patterns, and which have model parameters within the observed range. The performance of the models over this region is recorded in Table 1. For some models where the statistical parameters were found to deviate significantly from the observed parameter ranges, the subsequent checks of seasonal cycles, spatial patterns and the threshold values for the selected 100-year return period were not attempted. These instances are indicated by ‘not explored’ in Tables 1 and 2.

Table1. *Evaluation results for the climate models considered for the attribution analysis of the 60-day rainfall over the Indus river basin. The table contains qualitative assessments of seasonal cycle and spatial pattern of precipitation from the models (good, reasonable, bad) along with estimates for dispersion parameter, shape parameter and event magnitude. The corresponding estimates for observations are shown in blue. Based on overall suitability, the models are classified as good, reasonable and bad, shown by green, yellow and red highlights, respectively.*

Observations	**Seasonal cycle**	**Spatial pattern**	**Dispersion**	**Shape parameter**	**Event magnitude**
CPC			0.331 (0.245 ... 0.378)	0.063 (-0.21 ... 0.31)	6.3
ERA5			0.237 (0.169 ... 0.279)	-0.074 (-0.25 ... 0.082)	6.5
IMERG			0.245 (0.151 ... 0.313)	0.12 (-0.27 ... 0.33)	7.0
Model					**Threshold for 100-yr** return period
ECEARTHr12-COSMOcrCLIM ()	good	good	0.169 (0.137 ... 0.193)	-0.17 (-0.33 ... -0.045)	5.2
MIROCr1-REGCM ()	bad	good	0.196 (0.157 ... 0.228)	-0.096 (-0.29 ... 0.11)	4.9
MPIr1-COSMOcrCLIM ()	good	good	0.183 (0.137 ... 0.218)	-0.14 (-0.35 ... 0.15)	4.7
MPIMRr1-REGCM ()	good	good	0.197 (0.160 ... 0.227)	-0.096 (-0.79 ... 0.10)	5.8
MPIr1-REMO ()	good	good	0.203 (0.148 ... 0.243)	-0.15 (-0.40 ... 0.19)	3.4
NORESMr1-COSMOcrCLIM reasonable ()	good	good	0.192 (0.158 ... 0.223)	-0.060 (-0.28 ... 0.12)	5.6
NORESMr1-REGCM ()	good	good	0.191 (0.149 ... 0.221)	-0.023 (-0.24 ... 0.17)	6.4
NORESMr1-REMO ()	good	good	0.253 (0.175 ... 0.296)	0.063 (-0.14 ... 0.48)	5.6
GFDL/FLOR historical-rcp4.5 (10)	bad	good	0.163 (0.153 ... 0.172)	-0.056 (-0.10 ... -0.0080)	3.0
CANESMr1-RCA ()	bad	bad	0.290 (0.237 ... 0.329)	-0.019 (-0.36 ... 0.11)	2.1
CNRMr1-RCA ()	good	good	0.292 (0.236 ... 0.336)	-0.28 (-0.49 ... -0.11)	6.8
MK3r1-RCA ()	bad	bad	0.221 (0.173 ... 0.259)	0.11 (-0.10 ... 0.30)	2.9
ECEARTHr12-RCA ()	good	good	0.372 (0.314 ... 0.426)	-0.019 (-0.20 ... 0.16)	5.6
IPSLr1-RCA ()	reasonable	good	0.304 (0.242 ... 0.364)	0.30 (-0.0030 ... 0.60)	5.1
MIROCr1-RCA ()	good	good	0.306 (0.247 ... 0.347)	0.093 (-0.14 ... 0.27)	4.2
HADGEMr1-RCA ()	good	good	0.293 (0.226 ... 0.338)	0.17 (0.0020 ... 0.34)	4.8
MPIr1-RCA ()	good	good	0.304 (0.235 ... 0.351)	0.056 (-0.13 ... 0.25)	4.4
NORESMr1-RCA ()	good	good	0.322 (0.259 ... 0.367)	0.11 (-0.065 ... 0.29)	5.3
GFDLr1-RCA ()	good	good	0.246 (0.206 ... 0.276)	-0.14 (-0.34 ... 0.13)	3.7

CANESMr1-REGCM ()	<not explored>	<not explored>	0.132 (0.105 ... 0.152)	-0.17 (-0.43 ... -0.047)	<not explored>
CNRMr1-REGCM ()	<not explored>	<not explored>	0.137 (0.110 ... 0.159)	-0.20 (-0.37 ... -0.065)	<not explored>
MK3r1-REGCM ()	<not explored>	<not explored>	0.144 (0.112 ... 0.168)	-0.18 (-0.34 ... -0.038)	<not explored>
IPSLLRr1-REGCM ()	reasonable	reasonable	0.164 (0.124 ... 0.192)	-0.080 (-0.23 ... 0.13)	7.8
MPIMRr1-REGCM ()	<not explored>	<not explored>	0.123 (0.0930 ... 0.147)	-0.12 (-0.43 ... 0.18)	<not explored>
GFDLr1-REGCM ()	reasonable	reasonable	0.210 (0.172 ... 0.242)	-0.20 (-0.42 ... -0.014)	10.3
CNRM-CM6-1-HR HighResMIP ()	good	good	0.261 (0.204 ... 0.305)	-0.21 (-0.41 ... -0.083)	9.0
CMCC-CM2-VHr4 HighResMIP ()	reasonable	good	0.158 (0.125 ... 0.179)	-0.32 (-0.44 ... -0.14)	9.7
EC-Earth3P-HR HighResMIP ()	good	good	0.240 (0.185 ... 0.285)	-0.26 (-0.47 ... -0.090)	7.4
HadGEM3-GC31-HM HighResMIP ()	bad	reasonable	0.183 (0.144 ... 0.211)	-0.13 (-0.31 ... -0.014)	4.5
HadGEM3-GC31-MM HighResMIP ()	bad	reasonable	0.213 (0.170 ... 0.241)	-0.15 (-0.41 ... 0.038)	4.3
MPI-ESM1-2-XR HighResMIP ()	good	good	0.204 (0.168 ... 0.229)	-0.12 (-0.28 ... 0.019)	6.9

4.2 Balochistan and Sindh provinces

For the short-duration extreme 5-day rainfall event, only 11 of the 24 CORDEX are selected using our criteria. Many simulations cannot reproduce the ratio between variability and average rainfalls. In addition a few models exhibit a strong wet bias or a seasonal cycle not in agreement with observations. High-resolution models generally reproduce better statistics than low-resolution models. The FLOR ensemble could not be selected as it was unable to reproduce the statistical fit parameters. Out of the six HighResMIP models that were tested for the study, none was able to sufficiently capture the seasonal and spatial patterns, and have model parameters within the observed range. The performance of the models over this region is recorded in Table 2.

Table2. *Evaluation results for the climate models considered for the attribution analysis of the 5-day rainfall over Balochistan and Sindh provinces. The table contains qualitative assessments of seasonal cycle and spatial pattern of precipitation from the models (good, reasonable, bad) along with estimates for dispersion parameter, shape parameter and event magnitude. The corresponding estimates for observations are shown in blue. Based on overall suitability, the models are classified as good, reasonable and bad, shown by green, yellow and red highlights, respectively.*

Observations	Seasonal cycle	Spatial pattern	Dispersion	Shape parameter	Event magnitude
CPC			0.636 (0.487 ... 0.745)	0.092 (-0.14 ... 0.21)	19.0
IMERG			0.643 (0.406 ... 0.767)	0.070 (-0.23 ... 0.23)	22.3
ERA5			0.709 (0.579 ... 0.818)	-0.064 (-0.24 ... 0.12)	19.0
Model					**Threshold for 100-yr return period**
ECEARTHr12-COSMOcrCLIM ()	good	good	0.439 (0.368 ... 0.495)	-0.16 (-0.49 ... 0.042)	15.3
MIROCr1-REGCM ()	good	good	0.519 (0.402 ... 0.612)	-0.18 (-0.39 ... -0.0010)	17.7
MPIr1-COSMOcrCLIM ()	good	good	0.686 (0.585 ... 0.757)	0.18 (-0.25 ... 0.53)	25.1
MPIr1-REGCM ()	good	good	0.393 (0.290 ... 0.466)	-0.24 (-0.57 ... -0.0090)	17.7
MPIr1-REMO ()	good	good	0.619 (0.481 ... 0.734)	-0.24 (-0.56 ... 0.020)	18
NORESMr1-COSMOcrCLIM ()	good	good	0.931 (0.792 ... 1.02)	0.47 (0.032 ... 0.83)	69.1
NORESMr1-REGCM ()	good	good	0.668 (0.538 ... 0.760)	-0.032 (-0.34 ... 0.28)	24.7
NORESMr1-REMO ()	good	good	0.768 (0.615 ... 0.872)	-0.019 (-0.43 ... 0.48)	24
GFDL/FLOR historical-rcp4.5 (10)	bad	good	0.797 (0.754 ... 0.837)	0.44 (0.37 ... 0.50)	9.5
CANESMr1-RCA ()	0.564	0.761	0.506 (0.230 ... 0.843)	0.51 (0.23 ... 0.84)	12.9
CNRMr1-RCA ()	0.366	0.564	-0.312 (-0.708 ... -0.213)	-0.31 (-0.71 ... -0.21)	21
MK3r1-RCA ()	0.342	0.468	0.395 (0.0730 ... 0.667)	0.40 (0.073 ... 0.67)	4.9
ECEARTHr12-RCA ()	0.702	0.908	0.563 (0.126 ... 0.990)	0.56 (0.13 ... 0.99)	56.7
IPSLr1-RCA ()	0.739	0.982	0.807 (0.452 ... 1.20)	0.81 (0.45 ... 1.2)	53.7
MIROCr1-RCA ()	0.523	0.726	0.531 (0.271 ... 0.892)	0.53 (0.27 ... 0.89)	27
HADGEMr1-RCA ()	0.566	0.782	0.519 (0.209 ... 1.19)	0.52 (0.21 ... 1.2)	31
MPIr1-RCA ()	0.503	0.668	0.159 (-0.142 ... 0.402)	0.16 (-0.14 ... 0.40)	17.3
NORESMr1-RCA ()	0.562	0.728	0.285 (-0.00800 ... 0.551)	0.28 (-0.0080 ... 0.55)	26.1
GFDLr1-RCA ()	0.53	0.725	0.135 (-0.117 ... 0.353)	0.14 (-0.12 ... 0.35)	27.9
CANESMr1-REGCM ()	<not explored>	<not explored>	0.266 (0.207 ... 0.313)	-0.19 (-0.37 ... -0.035)	<not explored>
CNRMr1-REGCM ()	<not explored>	<not explored>	0.196 (0.156 ... 0.227)	-0.027 (-0.25 ... 0.16)	<not explored>

MK3r1-REGCM ()	<not explored>	<not explored>	0.409 (0.329 ... 0.471)	-0.19 (-0.34 ... -0.047)	<not explored>
IPSLLRr1-REGCM ()	<not explored>	<not explored>	0.189 (0.160 ... 0.212)	-0.061 (-0.24 ... 0.12)	<not explored>
MPIMRr1-REGCM ()	<not explored>	<not explored>	0.240 (0.192 ... 0.282)	-0.11 (-0.24 ... 0.057)	<not explored>
GFDLr1-REGCM ()	<not explored>	<not explored>	0.300 (0.234 ... 0.350)	-0.049 (-0.21 ... 0.11)	<not explored>
CNRM-CM6-1-HR HighResMIP ()	good	good	0.375 (0.288 ... 0.449)	-0.28 (-0.41 ... -0.15)	34.9
CMCC-CM2-VHr4 HighResMIP ()	reasonable	good	0.294 (0.213 ... 0.350)	-0.23 (-0.47 ... -0.092)	43.7
EC-Earth3P-HR HighResMIP ()	good	good	0.341 (0.266 ... 0.399)	-0.35 (-0.57 ... -0.15)	18.5
HadGEM3-GC31-HM HighResMIP ()	bad	reasonable	0.685 (0.574 ... 0.771)	0.34 (0.19 ... 0.46)	9.4
HadGEM3-GC31-MM HighResMIP ()	bad	reasonable	0.630 (0.533 ... 0.707)	0.26 (0.045 ... 0.41)	7.2
MPI-ESM1-2-XR HighResMIP ()	good	good	0.278 (0.224 ... 0.318)	-0.34 (-0.53 ... -0.24)	17.0

5 Multi-method multi-model attribution

This section shows Probability Ratios and change in intensity ΔI for models and also includes the values calculated from the fits with observations. Results are shown for both event definitions and for the current climate relative to a 1.2℃ cooler climate (before anthropogenic climate change) as well as a future 2.0℃ climate relative to the current climate.

***Table 3**. Threshold values of the 60-day rainfall over the Indus river basin for the selected return period of 1-in-100 years in the current, 2022 climate, along with the Probability Ratios and the change in intensities between the current climate and the pre-industrial, 1.2°C cooler climate (before anthropogenic climate change), for the observed datasets and the models that passed validation.*

Model / Observations	**Threshold for return period 100 yr** (mm/day)	**Probability ratio PR**	**Change in intensity ΔI [%]**
CPC	6.3	4.4e+2 (14 ... ∞)	1.2e+2 (16 ... 3.3e+2)
ERA5	6.5	0.77 (0.00073 ... ∞)	-2.3 (-35 ... 43)
IMERG	7.0	25 (0.0084 ... ∞)	68 (-34 ... 4.2e+2)
ECEARTHr12-COSMOcrCLIM ()	5.2	0.43 (0.0 ... ∞)	-4.6 (-17 ... 3.1)
MPIr1-COSMOcrCLIM ()	4.7	0.24 (0.0 ... ∞)	-9.7 (-21 ... -2.5)
MPIMRr1-REGCM ()	5.8	0.14 (0.0 ... ∞)	-16 (-30 ... 6.2)
MPIr1-REMO ()	3.4	0.28 (0.0 ... ∞)	-8.5 (-26 ... 10)
NORESMr1-COSMOcrCLIM reasonable ()	5.6	1.5 (0.090 ... ∞)	3.4 (-18 ... 3.9)

NORESMr1-REGCM ()	6.4	33 (2.1 ... ∞)	32 (4.3 ... 11)
NORESMr1-REMO ()	5.6	3.0 (0.33 ... ∞)	16 (-16 ... 20)
CNRMr1-RCA ()	6.8	∞ (9.8 ... ∞)	24 (-0.30 ... 55)
ECEARTHr12-RCA ()	5.6	0.26 (0.010 ... 2.1)	-18 (-37 ... 8.5)
IPSLr1-RCA ()	5.1	2.2 (1.2 ... 2.4e+2)	27 (7.9 ... 75)
MIROCr1-RCA ()	4.2	1.1 (0.010 ... 7.8)	2.0 (-23 ... 31)
HADGEMr1-RCA ()	4.8	1.7 (0.66 ... 12)	12 (-10 ... 42)
MPIr1-RCA ()	4.4	0.27 (0.020 ... 1.4)	-19 (-36 ... 4.6)
NORESMr1-RCA ()	5.3	2.4 (0.40 ... 2.1e+2)	17 (-14 ... 63)
GFDLr1-RCA ()	3.7	29 (0.36 ... 0.0)	19 (-7.4 ... 49)
IPSLLRr1-REGCM ()	7.8	2.9 (0.33 ... 1.4e+2)	7.1 (-4.6 ... 20)
GFDLr1-REGCM ()	10	0.16 (0.0 ... ∞)	-11 (-27 ... 5.0)
CNRM-CM6-1-HR HighResMIP ()	9.0	0.36 (0.0012 ... ∞)	-6.4 (-23 ... 14)
CMCC-CM2-VHr4 HighResMIP ()	9.7	0.14 (0.00079 ... ∞)	-7.5 (-17 ... 4.5)
EC-Earth3P-HR HighResMIP ()	7.4	2.9 (0.011 ... ∞)	4.2 (-20 ... 24)
MPI-ESM1-2-XR HighResMIP ()	6.9	0.87 (0.0057 ... 4.7e+2)	-0.98 (-19 ... 20)

Table 4. *Same as Table 3, but the Probability Ratios and the change in intensities between the current climate and a future climate with an additional warming of 0.8°C (before anthropogenic climate change), for the models that passed validation.*

Model	**Threshold for return period 100 yr (mm/day)**	**Probability ratio PR [-]**	**Change in intensity ΔI [%]**
ECEARTHr12-COSMOcrCLIM ()	5.2	0.58 (0.010 ... 1.6)	-2.6 (-7.2 ... 2.0)
MPIr1-COSMOcrCLIM ()	4.7	0.38 (0.0 ... 0.81)	-5.7 (-9.9 ... -1.7)
MPIMRr1-REGCM ()	5.8	0.80 (0.16 ... 1.6)	-1.9 (-8.5 ... 3.9)
MPIr1-REMO ()	3.4	1.0 (0.25 ... 2.6)	0.30 (-6.6 ... 6.4)
NORESMr1-COSMOcrCLIM reasonable ()	5.6	0.71 (0.32 ... 1.3)	-3.6 (-9.0 ... 2.5)
NORESMr1-REGCM ()	6.4	1.0 (0.23 ... 2.7)	0.20 (-6.3 ... 6.4)
NORESMr1-REMO ()	5.6	1.3 (0.77 ... 2.8)	4.2 (-4.1 ... 12)
CNRMr1-RCA ()	6.8	3.4 (0.99 ... 17)	7.5 (1.0 ... 14)
ECEARTHr12-RCA ()	5.6	0.96 (0.28 ... 1.7)	-0.70 (-11 ... 8.8)
IPSLr1-RCA ()	5.1	1.4 (1.2 ... 2.1)	12 (7.4 ... 17)
MIROCr1-RCA ()	4.2	1.4 (0.82 ... 2.6)	6.3 (-2.9 ... 15)
HADGEMr1-RCA ()	4.8	1.8 (1.3 ... 3.5)	11 (5.6 ... 15)
MPIr1-RCA ()	4.4	0.63 (0.27 ... 1.2)	-6.4 (-16 ... 1.9)
NORESMr1-RCA ()	5.3	1.3 (0.78 ... 2.4)	4.2 (-3.9 ... 12)
GFDLr1-RCA ()	3.7	3.0 (0.92 ... 26)	8.4 (0.0 ... 15)
IPSLLRr1-REGCM ()	7.8	1.8 (1.1 ... 5.6)	3.7 (0.53 ... 7.3)

Table 5. *Threshold values of the 5-day rainfall over the region encompassing Balochistan and Sindh provinces for the selected return period of 1-in-100 years in the current, 2022 climate, along with the Probability Ratios and the change in intensities between the current climate and a 1.2°C cooler climate (before anthropogenic climate change), for the observed datasets and the models that passed validation.*

Model / Observations	**Threshold for return period 100 yr (mm/day)**	**Probability ratio PR [-]**	**Change in intensity ΔI [%]**
CPC	19.036	64 (0.21 ... ∞)	1.1e+2 (-24 ... 4.5e+2)
IMERG	22.266	2.0e+2 (0.0000031 ... ∞)	1.3e+2 (-84 ... 3.6e+3)
ERA5	18.955	2.2 (0.0069 ... ∞)	11 (-38 ... 85)
ECEARTHr12-COSMOcrCLIM ()	15	0.13 (0.0 ... ∞)	-21 (-42 ... 9.5)
MIROCr1-REGCM ()	18	0.24 (0.0 ... ∞)	-14 (-40 ... 40)
MPIr1-COSMOcrCLIM ()	25	1.2 (0.14 ... ∞)	4.0 (-39 ... 70)
MPIr1-REMO ()	18	1.9 (0.010 ... ∞)	4.7 (-34 ... 67)
NORESMr1-REGCM ()	25	52 (0.37 ... ∞)	56 (-16 ... 1.8e+2)
NORESMr1-REMO ()	24	11 (0.15 ... ∞)	37 (-24 ... 1.9e+2)
CNRMr1-RCA ()	21	∞ (0.14 ... ∞)	21 (-6.1 ... 60)
HADGEMr1-RCA ()	31	2.0 (0.68 ... 17)	46 (-19 ... 1.7e+2)
MPIr1-RCA ()	17	0.40 (0.020 ... 8.4)	-21 (-48 ... 29)
NORESMr1-RCA ()	26	3.2 (0.44 ... 3.8e+2)	47 (-20 ... 1.6e+2)
GFDLr1-RCA ()	28	4.3 (0.090 ... 4.0e+4)	38 (-31 ... 1.8e+2)

Table 6. *Same as Table 5, but the Probability Ratios and the change in intensities between the current climate and a future climate with an additional warming of 0.8°C (before anthropogenic climate change), for the models that passed validation.*

Model	**Threshold for return period 100 yr**	**Probability ratio PR [-]**	**Change in intensity ΔI [%]**
MPIr1-COSMOcrCLIM ()	25.1	1.2 (0.18 ... 21)	4.7 (-38 ... 32)
NORESMr1-REGCM ()	24.7	5.0 (0.0 ... 1.4e+2)	25 (-12 ... 50)
NORESMr1-REMO ()	24	3.2 (0.0 ... 2.0e+2)	19 (-19 ... 50)
HADGEMr1-RCA ()	31	1.4 (1.1 ... 2.0)	18 (5.9 ... 28)
MPIr1-RCA ()	17.3	0.91 (0.36 ... 2.4)	-2.0 (-21 ... 13)
NORESMr1-RCA ()	26.1	1.3 (0.65 ... 3.0)	8.0 (-14 ... 25)
GFDLr1-RCA ()	27.9	1.4 (0.55 ... 4.0)	9.1 (-15 ... 28)

6 Hazard synthesis

For the event definitions described above we evaluate the influence of anthropogenic climate change on the event by calculating the probability ratio as well as the change in intensity using observations (in this case reanalysis data ERA5, and the two observational products CPC & IMERG) and models. Models which do not pass the validation tests described above are excluded from the analysis. The aim is to synthesise results from models that pass the evaluation along with the observations, to give an overarching attribution statement. Observations and models are combined into a single result in two ways if they seem to be compatible. Firstly, we neglect common model uncertainties beyond the model spread that is depicted by the model average, and compute the weighted average of models and observations: this is indicated by the magenta bar in Figs. 13 & 14. As, due to common model uncertainties, model uncertainty can be larger than the model spread, secondly, we also show the more conservative estimate of an unweighted average of observations and models, indicated by the white box around the magenta bar in the synthesis figures.
For both event definitions only few models pass the evaluation. The remaining models as well as the three observational products show very differing results and very large uncertainties. Due to these large uncertainties as well as the lack of structural diversity in the remaining models we refrain from quantifying the role of anthropogenic climate change. For the 60-day and the 5-day extreme rainfall, the majority of models do show an increase in likelihood (right panels in Figs. 13 & 14) and intensity (left panels in Figs. 13 & 14) that is potentially very large, with best estimates of a change in intensity of up to 30% for the large region (Fig. 13(*left*)) and up to 50% for the small region (Fig. 14(*left*)), respectively.

As a conclusion, models are unable to provide a basis to confidently quantify the change in the monsoon season rainfall intensity with climate change up to now. Qualitative statements are however possible.

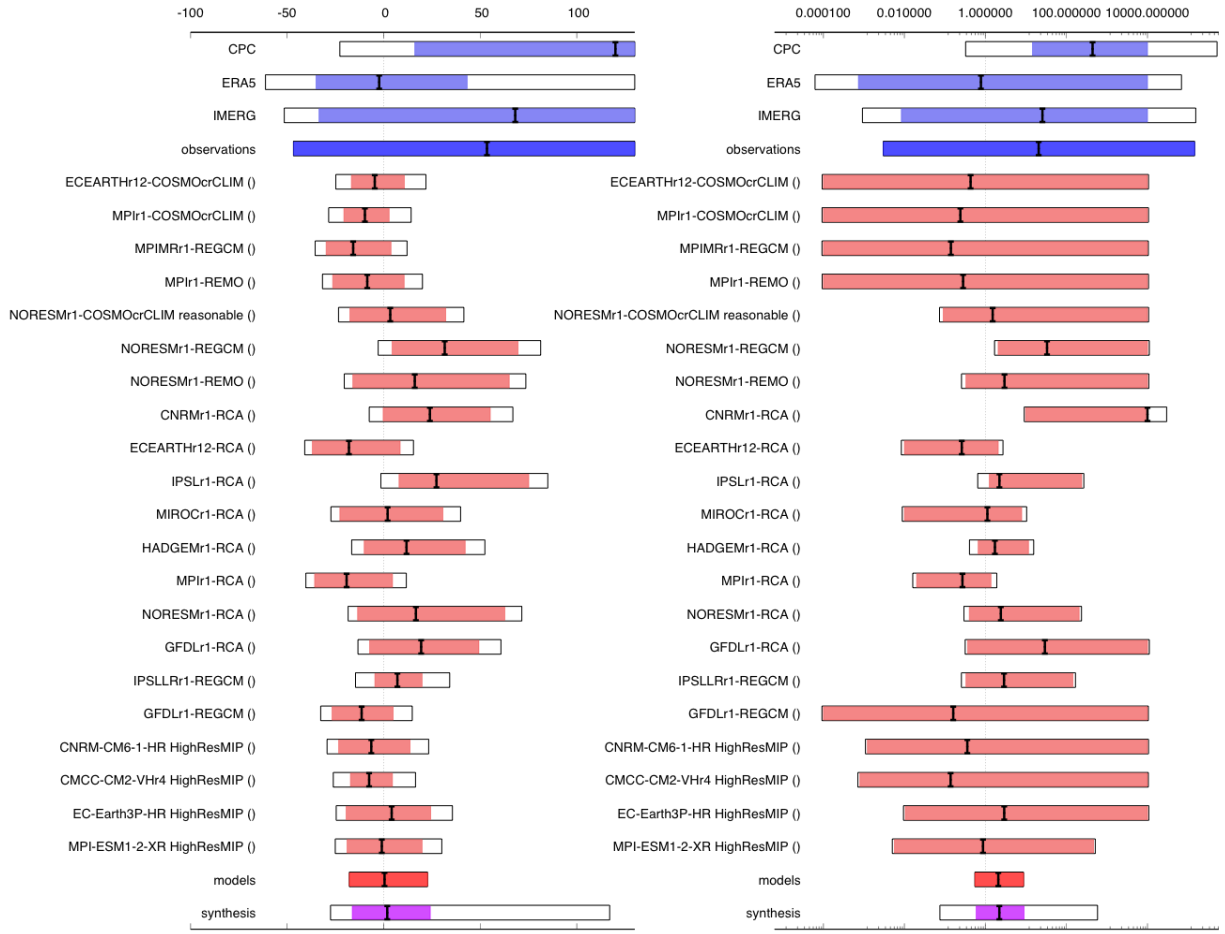

Figure 13. *Synthesis of intensity change (left) and probability ratios (right), when comparing the 100-year 60-day heavy rainfall event over the Indus river basin with a 1.2C cooler climate.*

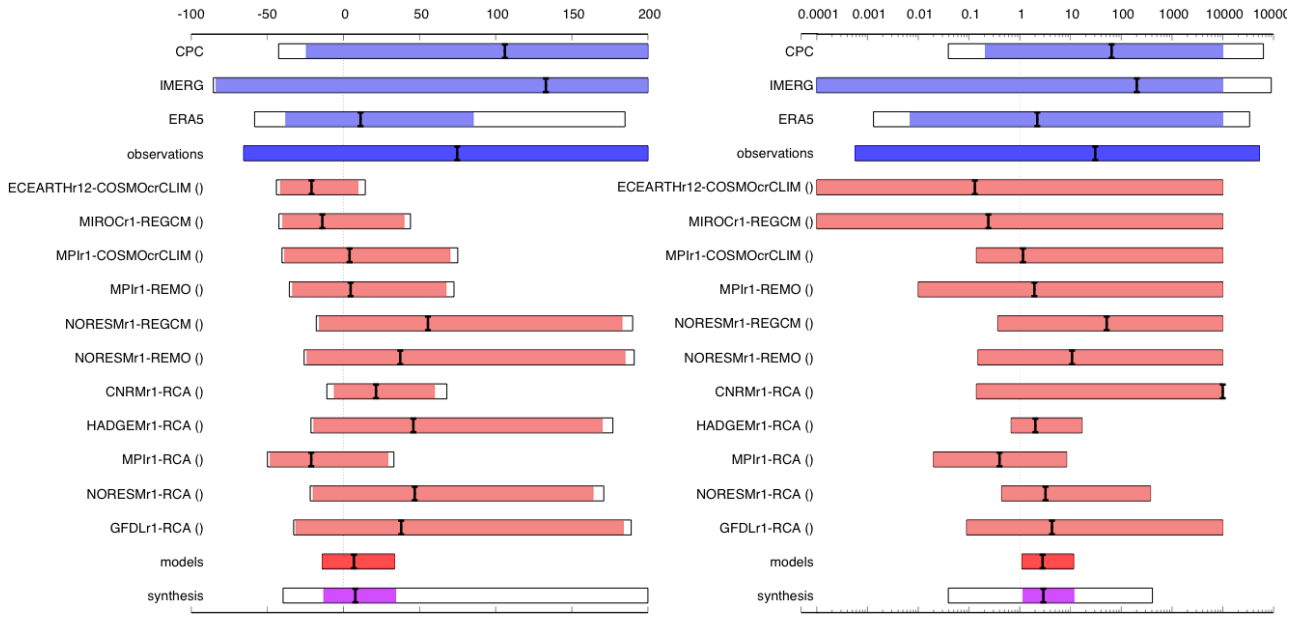

Figure 14. *Synthesis of intensity change (left) and probability ratios (right), when comparing the 100-year 5-day heavy rainfall event over the region encompassing Balochistan and Sindh, with a 1.2C cooler climate.*

Projecting the changes in likelihood and intensity for a 0.8℃ warmer future, Figs. 15 & 16 again show large discrepancies between the models. Despite this, models project a statistically significant change for the short-duration event with intensities increasing by 13% (Fig. 16 (*left*)) and probabilities increasing by 40% (Fig. 16 (*right*)). This increase is compatible with but slightly larger than what we expect from the Clausius-Clapeyron relationship. We note that these projected changes are on average smaller than those in the published literature for the region (e.g. Gutierrez et al., 2021). This adds more confidence to the models projecting a high increase. Given however that the literature in general encompasses a larger region with less natural variability this is not surprising, but renders reliable quantitative projections difficult.

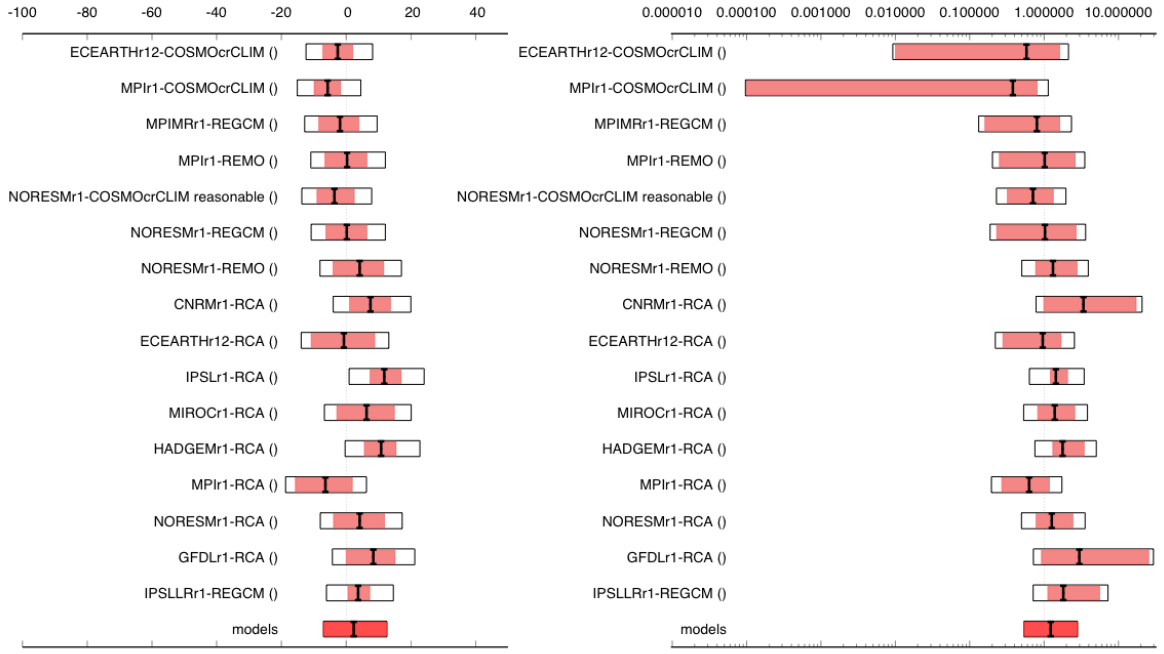

Figure 15. *Synthesis of intensity change (left) and probability ratios (right), when comparing the 100-year 60-day heavy rainfall event over the Indus river basin with a with a 0.8C warmer climate (2C since pre-industrial).*

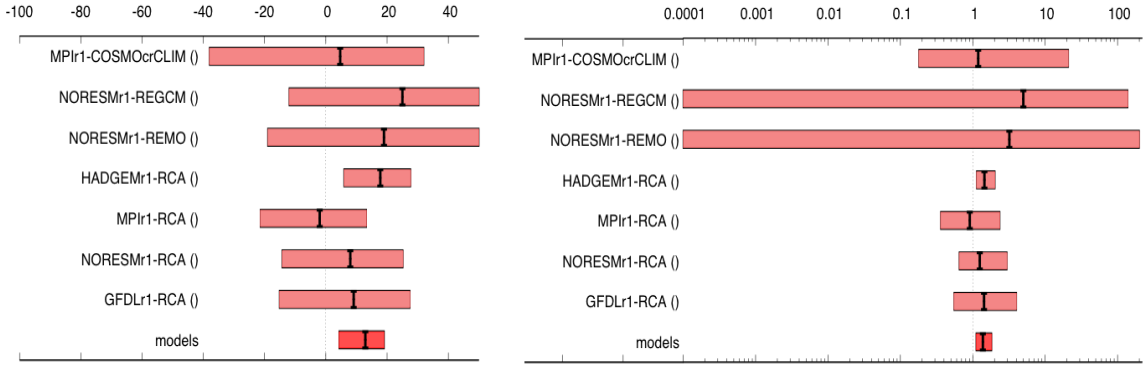

Figure 16. *Synthesis of intensity change (left) and probability ratios (right), when comparing the 100-year 5-day heavy rainfall event over the region encompassing Balochistan and Sindh, with a 0.8C warmer climate (2C since pre-industrial).*

7 Vulnerability and exposure

The devastating floods in Pakistan immediately made global headlines, with media suggesting that the event is a consequence of "a monsoon on steroids"[1], "erupting glaciers"[2] and "record rainfall"[3]. While a confluence of these physical events was involved in the production of this disaster, this section examines some of the factors of exposure and vulnerability of the people and communities impacted by the hazard that increased or decreased the impact of the extreme rain.

The Pakistan Meteorological Department (PMD) figures suggest that the two most impacted provinces, Sindh and Balochistan, received 726 percent and 590 percent of average August rainfall. While it is fair to say that rainfall was exceptionally high, heavy rains and extensive flooding were also experienced by the country in the recent past, for example 2010, 2011 and 2012 (Rasmussen et al., 2015). Pakistan receives most of its rainfall during the monsoon season and thus flooding patterns in Pakistan are predictable. The worst impacts are usually felt as a result of May-August (MJJA) rainfall (Webster et al., 2011), downstream areas of the Indus River are normally the worst affected and small towns and villages away from urban centres are inundated with water, especially in the province of Sindh (Ali, Mannakkara and Wilkinson, 2020; Busby et al., 2018; Syvitski and Brakenridge, 2012). Despite this knowledge, addressing the structural causes of vulnerability and exposure, especially in downstream Pakistan, remains a significant challenge.

Water management along the Indus Delta

Pakistan already experienced catastrophic flooding in 2010. Subsequent studies (for example, the Report of the Flood Inquiry commissioned by the Supreme Court, see Khan, 2011; Mustafa and Wrathall, 2011) have concluded that it was not just the result of exceptional weather events but rather "that most damage was caused by dam and barrage-related backwater effects, reduced water and sediment conveyance capacity, and multiple failures of irrigation system levees" (Syvitski and Brakenridge, 2012, p. 4) . Further, this research also suggests that reinforcing existing engineering structures would not prevent future flooding and warned that such a flooding disaster was certain to take place during future rains (Syvitski and Brakenridge, 2012). These findings illustrate two wider and significant causes

[1] https://edition.cnn.com/2022/08/29/asia/pakistan-flood-damage-imf-bailout-intl-hnk/index.html
[2] https://edition.cnn.com/2022/08/29/asia/pakistan-flood-damage-imf-bailout-intl-hnk/index.html
[3] https://time.com/6209967/pakistan-floods-what-to-know/

of vulnerability and exposure in towns and villages along the Indus Delta. First, a river development paradigm pursued by state planners based on engineering-driven interventions to harness water as a "resource" with little regard for local environments (Akhter 2015; Aijaz and Akhter, 2020; Akhter, 2022). Secondly, reliance on an irrigation management system first constructed by the British Raj to meet other political and state-building ends rather than providing a channel for equitable water distribution (Gilmartin, 1994; Mustafa, 2007; Haines, 2013).

The areas affected by the floods were preliminary rural (64% of the population lives in rural areas) farmlands. Agriculture is an important part of Pakistan's economy, accounting for 26% of GDP (Rehman et al., 2015). The Indus river provides water for nearly 90 percent of food production in Pakistan, and thirty-nine percent of the country's labour force is engaged in agriculture with wheat, rice, cotton and sugar cane being the primary crops[4]. It is the people who depend on agriculture who have been most vulnerable in the face of these floods. This reveals some of the issues with the way water is channelled and diverted, contributing to exposure and vulnerability of communities living amidst these hydraulic systems.

State policy in Pakistan has been to rely on a river engineering paradigm and hydrological mega projects for flood management. This has tended to create a number of drainage problems followed by more technical solutions in the Basin (Mustafa and Wrathall, 2010). The lower Indus Basin, for example, has been known to be vulnerable to drainage "failures", even during non-flood years (Basharat and Rizvi, 2016), leaving it particularly exposed in the face of high-intensity rainfall. At one level, while large-scale and highly engineered drainage projects have been constructed (such as the Right Bank Outfall Drain [RBOD] and the Left Bank Outfall Drain [LBOD]) to drain irrigation water out into the sea, the problems associated with these projects are well documented (Gonzalez-Villareal, 2001; Mahessar et al., 2019). The back-up of drainage flows on the LBOD was responsible for flooding large parts of Badin District in Sindh in 2010 (Siddiqi, 2019). More generally, long-term reduction in watercourse channel capacity in these hydraulic systems due to sedimentation was also considered a key reason exacerbating those floods (Mustafa and Wrathall, 2010). Beyond engineering problems or failures, there is also wider conversation taking place on whether Pakistan's ideological bias towards modernist engineering solutions (Akhter et al., 2022) needs to be re-considered in favour of a more decolonial approach (Mustafa, 2022).

Since the early twentieth century, floods along the River Indus have been managed by breaching of levees and intentionally spilling flood water (Asif et al., 2007; Mustafa and Rathall, 2011). Flood vulnerability is not only dependent on political power today, but also on historically contingent processes of social engineering – location of land in connection to water sources has been dependent on loyalty to Crown and state - undertaken by the colonial

4https://www.fao.org/pakistan/our-office/pakistan-at-a-glance/en/#:~:text=In%20total%2C%20the%20agriculture%20sector,densely%20populated%20forests%20and%20rangelands.

and post-colonial state (Mustafa et al., 2019). Similarly, diverting excess water to the countryside to protect cities is a policy continuing since British colonial rule (Mustafa and Rathall, 2011).

As a consequence of the nation's recurring floods and ensuing farmland devastation, evidence suggests that the agricultural sector is experiencing a shift from cash crops to livestock production (Jamshed et al., 2017). However, large farm animals are particularly vulnerable to drowning in floods and estimates on loss of livestock in Sindh are in the hundreds of thousands (Latif, 2022).

Disaster management policy and early warning systems

The primary policy framework for disaster preparedness and response is laid out in the National Disaster Management Act passed by Parliament in 2010, in part as a response to the devastating floods during that year (Ahmed, 2013). It follows a three-tier disaster management system that assigns roles and responsibilities for "preparedness, response, recovery and rehabilitation and reconstruction" to national, provincial and district level disaster management authorities[5]. This institutional architecture does not provide a roadmap for instituting disaster risk management at a local or community level. In an era of community based disaster risk management (CBDRM) and participatory disaster risk assessments (PDRA), Pakistan's disaster risk paradigm is centralised with limited avenues for hazard or vulnerability mapping to take place at local levels (as in countries such as Bangladesh or in The Philippines, see Fernandez, Uy and Shaw, 2012; Habiba, Shaw and Abedin, 2013). The resulting gulf between "policies at the top" and "voices at the bottom" has been documented in research (Mysorewalla, 2019).

In effect, the DDMA is rarely operationalised outside of when a disaster occurs (Forni et al., 2013). Issues such as low capacity and limited resource allocation, limited technical expertise in the public sector in a new area, and weak partnerships and convening power with other public sector entities limit the Provincial Disaster Management Authority's efficacy in preparedness and ex-ante risk reduction (Pakistan - Sindh Resilience Project, 2016).

In 2012, Pakistan launched its 10-year national disaster management plan, envisaging improvements including developing a multi-hazard early warning system (MHEWS) to cover riverine, flash, and glacial lake outburst floods. (NDMA, 2012; Mukhtar, 2018). In 2016 the World Bank launched a $120 million project in Sindh province to improve institutional capacity for disaster and climate risk management, increase the number of people receiving timely and more accurate early warning notifications, and establish a Sindh emergency service, among other activities intended to strengthen resilience to floods and droughts (World Bank, 2021). The project is slated to end in 2024, and has made progress including

[5] https://cms.ndma.gov.pk/storage/app/public/pages/September2020/NDMA-Act.pdf

preparing integrated disaster management plans for Sindh province, and upgrading and strengthening an emergency operations centre in the disaster management association, but as of 2021 there was no dedicated capacity to respond to emergencies by the Sindh emergency service (World Bank 2021). Reviews in the ensuing months will determine whether these investments were able to reduce impacts during the floods in 2022.

Analyses of Pakistan's broader framework for managing disasters often suggest that it is more reactive and while an early warning system (EWS) exists its delivery systems are unclear (Ali and Iqbal 2021; Cheema et al 2016), though local police stations and mosques have been used in the past (Mustafa et al., 2015). However, since 2021 there have been some improvements, notably with the World Bank Sindh Resilience project reporting seven million people now receive timely and more accurate early warning notifications (World Bank, 2021). It is also important to note that the "flash" nature of much of the flooding, and large amount of water may also have significantly limited the effectiveness of any early warnings even if the systems were in place.

Infrastructure

The heavy rainfall and ensuing floods damaged over 1.7 million homes, 6.700 kilometres of road, 269 bridges and 1.460 health facilities (NDMA, 2022; OCHA, 2022; Save the Children, 2022). Early estimates of this devastation suggest that it totals US$30 billion (Business Standard, 2022). Development in flood-prone areas is a factor that contributed to the high infrastructure damages during the current floods and policies that mandate flood zones that restrict building can be implemented to reduce this risk in the future (Mallapaty, 2022). Many of the homes damaged in the current floods were traditional (mud) structures, and upgrading to flood resistant ones (concrete) through support for rebuilding efforts and awareness raising could increase resilience to future floods (Shah et al., 2018).

According to initial assessments by the Pakistan Red Crescent Society (PRCS), the construction of a flood mitigation wall to limit flood damage to districts in KP such as Nowshera, Peshawar and Charsadda from floods, had positive effects during the 2022 floods. The PRCS found that despite the fact that the intensity of the current flooding was as high as the 2010 floods in this area, the damages would have been greater if the flood mitigation wall was not constructed. Similarly, the preparedness of disaster management authorities has also improved in some cases. Communities in Nowshera and Charsadda were evacuated 24 to 48 hours before the floodwater inundated the area which has contributed to a lower mortality rate in these areas. While these are anecdotal instances of risk reduction, and a full assessment of the impact of these interventions is required, they do point to the potential for improved risk reduction and early warning systems to reduce impacts on vulnerable people.

Household vulnerability

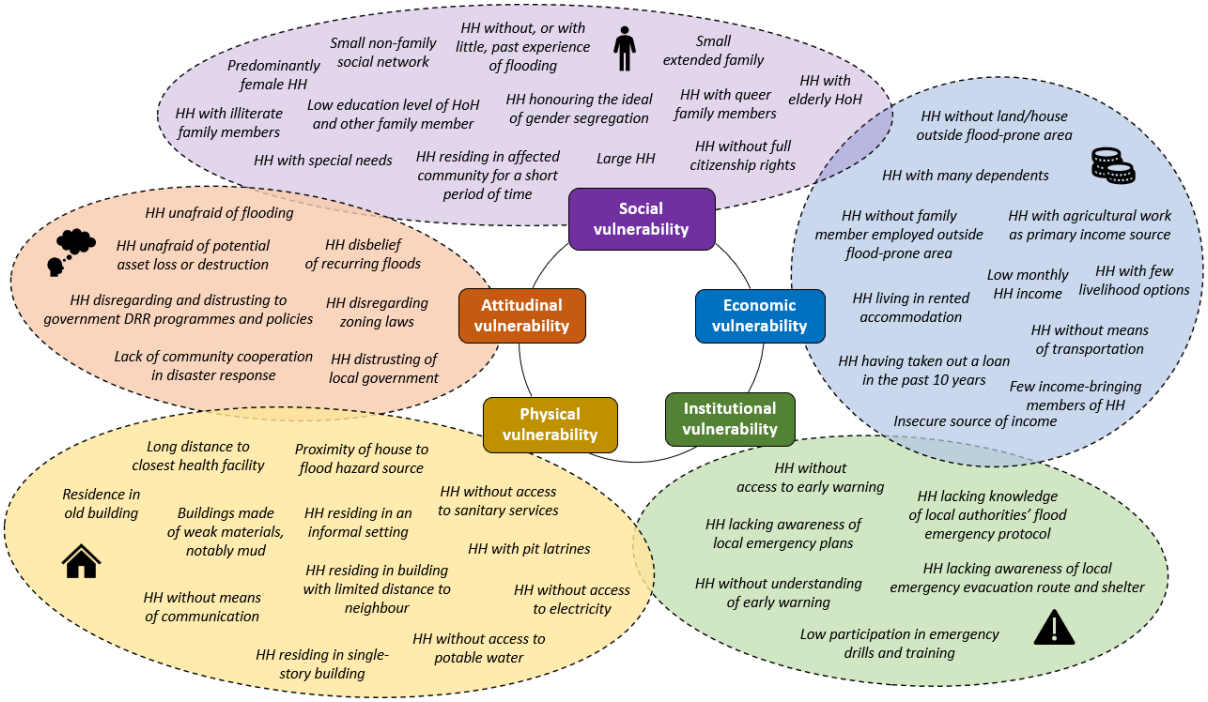

Figure 17. *A visual representation of household (HH) factors contributing to vulnerability to floods in Pakistan categorised by types of vulnerability developed in Rana and Routray (2018) based on empirical evidence and evidence from studies across Pakistan (Memon, 2020; Sadia et al., 2016; Anjum and Fraser, 2021; Mustafa et al., 2015; Ajani and van der Geest, 2021; Shah et al., 2020).*

A review of household flood vulnerability following the 2010 floods in Khyber Pakhtunkhwa (KP) province revealed that key factors affecting household's flood vulnerability included respondents' socio-economic and demographic attributes (e.g. age, gender, education, income), their house-construction material, past experience with floods and social networks (Shah et al., 2020). Other studies found similar results, including one that developed a multi-dimensional model for vulnerability based on empirical evidence and highlights social, economic, institutional, physical and attitudinal factors that contribute to vulnerability (Rana and Routray, 2018). Using this framework, and a literature review of studies across Pakistan on flood vulnerability, we developed figure 17 highlighting the many factors that can increase risk during floods.

Vulnerability manifests through various impact pathways, for example, poverty can result in households living in poorly constructed (mud) houses, in areas where land is cheaper and more flood-prone, and far from health facilities. These factors can combine with socioeconomic factors (e.g. income, education, livelihood sources) in direct and in-direct ways, leading to greater risks from floods (Shah et al., 2020). Access to health facilities, type of latrine, access to information, distance from the nearest health facility, health facilities impacted by 2010 flood, and damaged water supply infrastructure were also highlighted as

important factors affecting household vulnerability to floods (Rana and Routray, 2018). Waterborne illnesses are already affecting people who have survived the direct effects of the current floods, illustrating the importance of access to water, sanitation and hygiene, and nearby health facilities (Sarkar, 2022).

Women in Pakistan are more vulnerable to suffer the worst from the flood hazard because of their relative lack of mobility compared to men (Mustafa et al 2019). This largely stems from women's traditional role as primary caretaker for the elderly and children (Shah et al., 2020; Rana and Routray, 2018), but also the widespread ideal of purdah, gender segregation, which can incline women to stay at home rather than evacuating to a mixed-gender community shelter (Mustafa et al., 2015). Even when women are able to reach the safety of temporary shelters, such as flood settlement camps, they are vulnerable to physical violence (Memon, 2020).

To address this gender issue, Pakistan's flagship social protection programme, the Benazir Income Support Programme (BISP) makes cash transfers directly to women has had some success in addressing these forms of existing inequalities (Waqas and Awan, 2019; Naseer et al., 2021). The cash transfers after the floods in 2010 and 2011, were made to "heads of households", typically men through ATM cards (Watan card and Pakistan card). Despite numerous positive outcomes (Siddiqi, 2013, 2018), these programmes inadvertently marginalise households where the passing/absence of a usually male head is unrecorded, in turn, leaving women more vulnerable to non-payment of disaster relief. Severely marginalized, the country's transgender population is a notably vulnerable group (Mustafa et al., 2015).

Environmental challenges facing the Indus Delta

This flooding has taken place within a broader context of the slow degradation of the Indus Delta downstream. The various river diversions and different large-scale projects mentioned earlier have changed natural ecological systems along the river with significant impacts on the wider delta. The reduction of freshwater discharge and changing patterns and levels of salinity in the water have all been evidenced in research (Mahar and Zaigham, 2021; Wang et al., 2019; Khuhawar et al., 2018). These issues have produced various slow-onset disasters that include the changing environment of the delta, coastal erosion, intrusion of saline water, destruction of fertile land, shortage of drinking water, loss of mangrove vegetation, reduction in fish catch (Salman, 2011; Laghari et al., 2015). These regions and their communities are thus particularly vulnerable to any extreme weather event.

Vulnerability and exposure conclusion

In addition to the climatic hazard, the factors driving the devastating impacts for the 33 million people affected in Pakistan include the proximity of human settlements, infrastructure, and agricultural land to flood plains, limited ex-ante risk reduction capacity, an outdated river management system, underlying vulnerabilities driven by poverty, socioeconomic factors that disadvantage women, and ongoing political and economic instability. The extreme nature of the rainfall and subsequent floods means that some level of impact was likely unavoidable. The Pakistan government's established record in providing social protection interventions especially after disasters (World Bank, 2013), and ongoing projects to strengthen resilience to floods, may have played a role in reducing the impacts of the current floods. However, there are still critical gaps in the full implementation and operationalisation of disaster management policies and plans developed following the 2010 floods, that may reduce the impact of future floods. Rebuilding following the disaster also provides an opportunity to strengthen resilience and avoid future risk through stronger infrastructure designed for the new climate and considerations of flood risk when deciding where to rebuild.

Data availability

Almost all data are or will soon be available via the Climate Explorer.
For access to weather station data, please contact Pakistan Meteorological Department.

References

All references are hyperlinked in the main text.